The Functional Relationship between the Cdc50p-Drs2p Putative Aminophospholipid Translocase and the Arf GAP Gcs1p in Vesicle Formation in the Retrieval Pathway from Yeast Early Endosomes to the TGN

Hiroshi Sakane[1], Takaharu Yamamoto[1, 2], and Kazuma Tanaka[1, 2*]

Division of Molecular Interaction, Institute for Genetic Medicine, Hokkaido University Graduate Schools of [1]Medicine and [2]Life Science, N15 W7, Kita-ku, Sapporo 060-0815, Japan

Keywords: phospholipid asymmetry, endocytic recycling, Arf signaling, yeast

Running head: Phospholipid asymmetry and an Arf GAP

Phone: +81-11-706-5165

Fax: +81-11-706-7821

E-mail address: k-tanaka@igm.hokudai.ac.jp

[*]To whom correspondence should be addressed

Abbreviations used: AP, adaptor protein; APLT, aminophospholipid translocase; Arf, ADP-ribosylation factor; CCV, clathrin-coated vesicle; CPY, carboxypeptidase Y; EM, electron microscopy; ER, endoplasmic reticulum; GAP, GTPase-activating protein; GEF, guanine nucleotide exchange factor; GFP, green fluorescent protein; GGA, Golgi-localizing, γ-adaptin ear homology domain, Arf-binding protein; 3HA, three tandem repeats of the influenza virus hemagglutinin epitope; LAT-A, latrunculin A; mRFP1, monomeric red fluorescent protein 1; TGN, *trans*-Golgi network; ts, temperature-sensitive.

ABSTRACT

Drs2p, the catalytic subunit of the Cdc50p-Drs2p putative aminophospholipid translocase, has been implicated in conjunction with the Arf1 signaling pathway in the formation of clathrin-coated vesicles (CCVs) from the TGN. Herein, we searched for Arf regulator genes whose mutations were synthetically lethal with *cdc50Δ*, and identified the Arf GAP gene *GCS1*. Most of the examined transport pathways in the Cdc50p-depleted *gcs1Δ* mutant were nearly normal, including endocytic transport to vacuoles, carboxypeptidase Y sorting, and the processing and secretion of invertase. In contrast, this mutant exhibited severe defects in the early endosome-to-TGN transport pathway; proteins that are transported via this pathway, such as the v-SNARE Snc1p, the t-SNARE Tlg1p, and the chitin synthase III subunit Chs3p, accumulated in TGN-independent aberrant membrane structures. We extended our analyses to clathrin adaptors, and found that Gga1p/Gga2p and AP-1 were also involved in this pathway. The Cdc50p-depleted *gga1Δ gga2Δ* mutant and the *gcs1Δ apl2Δ* (the β1 subunit of AP-1) mutant exhibited growth defects and intracellular Snc1p-containing membranes accumulated in these cells. These results suggest that Cdc50p-Drs2p plays an important role in the Arf1p-mediated formation of CCVs for the retrieval pathway from early endosomes to the TGN.

Introduction

It is widely accepted that plasma membrane phospholipids are asymmetrically distributed in the two leaflets of the membrane bilayers in eukaryotic cells (Devaux, 1991). In this phospholipid asymmetry, phosphatidylethanolamine and phosphatidylserine are enriched in the inner leaflet facing the cytoplasm, whereas phosphatidylcholine, sphingomyelin, and glycolipids are predominantly found in the outer leaflet. The asymmetric distribution of phospholipids is generated and maintained by ATP-driven lipid transporters or translocases. The P4 subfamily of the P-type ATPases has been implicated in the translocation of aminophospholipids from the external to the cytosolic leaflet (Holthuis and Levine, 2005; Graham, 2004; Pomorski *et al*., 2004). In the yeast *Saccharomyces cerevisiae*, five members of this subfamily (Drs2p, Neo1p, Dnf1p, Dnf2p, and Dnf3p) are encoded by the genome (Hua *et al*., 2002; Catty *et al*., 1997). Drs2p is localized to the endosomal/*trans*-Golgi network (TGN) compartments (Saito *et al*., 2004; Pomorski *et al*., 2003; Hua *et al*., 2002; Chen *et al*., 1999), suggesting that Drs2p regulates the phospholipid asymmetry in these membranes. In fact, Golgi membranes isolated from a temperature-sensitive (ts) *drs2* mutant lacking *DNF1*, *DNF2*, and *DNF3* exhibited defects in the ATP-dependent transport of a fluorescent 7-nitrobenz-2-oxa-1,3-diazol-4-yl (NBD)-labeled analog of phosphatidylserine (Natarajan *et al*., 2004). Alder-Baerens *et al*. (2006) also demonstrated that post-Golgi secretory vesicles contained a Drs2p- and Dnf3p-dependent NBD-labeled phospholipid translocase activity and that the asymmetric phosphatidylethanolamine arrangement in these vesicles was disrupted in the *drs2Δ dnf3Δ* mutant.

We previously isolated *CDC50*, which encodes a conserved membrane-spanning protein, as a gene required for polarized cell growth (Misu *et al*., 2003). Cdc50p colocalized with Drs2p at endosomal/TGN membranes, and associated with

Drs2p as a putative non-catalytic subunit (Saito *et al*., 2004). In the absence of Cdc50p, Drs2p was observed in the endoplasmic reticulum (ER) due to a failure of the protein to exit the ER; a lack of Drs2p conversely led to the retention of Cdc50p in the ER. Both the *cdc50Δ* and *drs2Δ* mutants exhibited growth defects and depolarization of cortical actin patches at lower temperatures (Saito *et al*., 2004; Misu *et al*., 2003). This actin depolarization phenotype may be due to defects in the endocytic recycling pathway, because actin patches seemed to assemble on endocytosed membranes in the *cdc50Δ* mutant cultured at the low temperature and Cdc50p-depleted *erg3Δ* (a mutation in the gene that codes for sterol C-5 desaturase Erg3p, which catalyzes a late step in the ergosterol biosynthetic pathway) mutant (Kishimoto *et al*., 2005, our unpublished results). Thus, the functions of the Cdc50p-Drs2p complex in vesicle trafficking need to be investigated to understand how Cdc50p-Drs2p regulates the polarized organization of the actin cytoskeleton as well as polarized cell growth.

A mutation in *DRS2* was shown to cause synthetic lethality with a null mutation in *ARF1*, a gene that codes for an ADP-ribosylation factor (Arf) small GTPase (Chen *et al*., 1999). *ARF1* is part of an essential gene family that also includes *ARF2*, which produces a gene product that is 96% identical to Arf1p at the amino-acid sequence level, and *ARF1* produces approximately 90% of total Arf1p/Arf2p (Stearns *et al*., 1990), suggesting that Arf1p plays a major role. Arf proteins cycle between an inactive GDP-bound form and an active, membrane-associated GTP-bound form. Conversion from the GDP-bound to the GTP-bound form is facilitated by an Arf guanine nucleotide exchange factor (Arf GEF), whereas GTP hydrolysis is induced by an Arf GTPase-activating protein (Arf GAP) (reviewed in Donaldson and Jackson, 2000). Gea1p, Gea2p, Sec7p, and Syt1p have been identified as Arf GEFs in *S. cerevisiae* (reviewed in Jackson and Casanova, 2000). Gea1p and Gea2p play important roles in the

structure and function of the Golgi apparatus, and have overlapping functions in the Golgi-to-ER retrograde transport pathway (Peyroche *et al*., 2001; Spang *et al*., 2001). Sec7p is a Golgi-localized protein that is involved in the ER-Golgi and intra-Golgi transport pathways (Franzusoff *et al*., 1991, 1992). On the other hand, Gcs1p, Glo3p, Age1p, and Age2p have been identified as Arf GAPs in *S. cerevisiae* (Zhang *et al*., 2003; Poon *et al*., 2001; Dogic *et al*., 1999; Poon *et al*., 1996). Gcs1p functions redundantly with Glo3p in the Golgi-to-ER retrograde transport pathway (Poon *et al*., 1999), and with Age2p in transport from the TGN (Poon *et al*., 2001). Gcs1p is also involved in the organization of the actin cytoskeleton (Blader *et al*., 1999) and mitochondrial morphology (Huang *et al*., 2002).

Arf1p has been implicated in the formation of COPI-coated vesicles in the Golgi-to-ER retrograde transport pathway (Poon *et al*., 1999; Gaynor *et al*., 1998), and clathrin-coated vesicles (CCVs) in transport from the TGN (Chen and Graham, 1998). The *drs2Δ* mutation also causes synthetic lethality with a mutation in *CHC1*, which codes for the clathrin heavy chain (Chen *et al*., 1999), suggesting the involvement of Cdc50p-Drs2p in clathrin-associated vesicle transport. Indeed, the *drs2Δ* mutant exhibits TGN defects comparable with those exhibited by strains with clathrin mutations, and is defective in the formation of CCVs (Gall *et al*., 2002; Chen *et al*., 1999).

Clathrin adaptors may regulate the Arf-dependent formation of CCVs. These proteins link clathrin to membrane cargo, lipids, and accessory proteins that regulate coat assembly and disassembly. There are two known types of clathrin adaptors; the heteromeric adaptor protein (AP) complexes composed of four subunits, and the monomeric GGA (Golgi-localizing, γ-adaptin ear homology domain, Arf-binding protein) proteins. In *S. cerevisiae*, there are three AP complexes, AP-1, AP-2R, and AP-3 (Yeung *et al*., 1999), and two GGAs, Gga1p and Gga2p (Costaguta *et al*., 2001;

Dell'Angelica *et al*., 2000; Hirst *et al*., 2000). Both AP-1 and Gga1p/Gga2p physically interact with clathrin (Costaguta *et al*., 2001; Yeung and Payne, 2001; Yeung *et al*., 1999). It has been suggested that Gga1p and Gga2p are involved in the formation of CCVs in the TGN-to-late endosome transport pathway (Costaguta *et al*., 2001; Black and Pelham, 2000; Dell'Angelica *et al*., 2000; Hirst *et al*., 2000), although the interaction with Arf1p is not sufficient for the Golgi-localization and function of Gga1p/Gga2p (Boman *et al*., 2002). On the other hand, Arf1p and AP-1 have been implicated in the retrieval of the Chitin synthase III subunit Chs3p from early endosomes to the TGN (Valdivia *et al*., 2002).

In this study, in order to identify vesicle transport routes that involve the Cdc50p-Drs2p putative aminophospholipid translocase (APLT) and the Arf signaling pathway, we searched for *ARF*-related genes that genetically interact with *CDC50*, resulting in the identification of *GCS1*. The Cdc50p-depleted *gcs1Δ* mutant exhibited severe defects in the early endosome-to-TGN transport pathway, but not in other vesicle transport pathways. Similar phenotypes were found in the *gga* mutants depleted of Cdc50p, and in a mutant carrying the *gcs1Δ* mutation in combination with a mutation in AP-1. Our results raise the possibility that changes in phospholipid asymmetry are involved in the Arf-dependent formation of TGN-targeted CCVs from early endosomes.

Materials and Methods

Media and Genetic Techniques

Unless otherwise specified, strains were grown in YPDA rich medium (1% yeast extract [Difco, Detroit, MI], 2% bacto-peptone [Difco], 2% glucose, and 0.01% adenine). Strains carrying plasmids were selected in synthetic medium (SD) containing the required nutritional supplements (Rose *et al*., 1990). When appropriate, 0.5% casamino

acids (Difco) were added to SD medium without uracil (SDA-Ura). For induction of the *GAL1* promoter, 3% galactose and 0.2% sucrose were used as carbon sources instead of glucose. Standard genetic manipulations of yeast were performed as described previously (Guthrie and Fink, 1991). Yeast transformations were performed using the lithium acetate method (Gietz and Woods, 2002; Elble, 1992). DH5α and XL1-Blue *Escherichia coli* strains were used for the construction and amplification of plasmids.

Strains and Plasmids

Yeast strains used in this study are listed in Table I. The yeast YEF473 background strains carrying complete gene deletions (*CDC50*, *ARF1*, *ARF2*, *ARF3*, *GCS1*, *GLO3*, *GGA1*, *GGA2*, *GEA1*, and *GEA2*); *GAL1* promoter-inducible *CDC50* tagged with three tandem repeats of the influenza virus hemagglutinin epitope (3HA); enhanced green fluorescent protein (EGFP)-tagged *APL4*, *VPS10*, and *KEX2*; monomeric red fluorescent protein 1 (mRFP1)-tagged *SEC7*; and the yeast S288C background strains carrying complete gene deletions (*APL2*, *GCS1*, *GGA1*, and *GGA2*) were constructed by polymerase chain reaction (PCR)-based procedures as described previously (Longtine *et al*., 1998). All constructs produced by PCR-based procedures were verified by colony-PCR amplification to confirm that the replacements had occurred at the expected loci. The yeast S288C background strains carrying complete gene deletions (*arl1Δ*, *arl3Δ*, *age1Δ*, *age2Δ*, *syt1Δ*, *apl4Δ*, *apm1Δ*, *aps1Δ*, *apl5Δ*, *apl6Δ*, *apm3Δ*, and *aps3Δ*) were gifts from C. Boone (University of Toronto).

The plasmid pRS313-GCS1 was constructed by the gap-repair method. The 5'-upstream region from -820 to -353 and the 3'-downstream region from +1369 to +1893 of the *GCS1* gene were amplified by the PCR using the oligonucleotide primers

GCS1up-5 (5'-ATGGATCCCTACGTGAACCCTGGTGTCCTC-3') and GCS1up-3 (5'-TAGATATCTATGTGGGCCAGCAGGTACAGG-3'), and GCS1down-5 (5'-ATGATATCAGACCTGGGACAATCGTTATCC-3') and GCS1down-3 (5'-TACTCGAGCCGATAATGGCACCGTCTTTTG-3'), respectively. The 5'-upstream and the 3'-downstream PCR products were digested with restriction enzymes, and subcloned into the *Bam*HI-*Eco*RV and *Eco*RV-*Xho*I gaps of pRS313, respectively. The resulting plasmid was digested with *Eco*RV and introduced into YEF473, and the gap-repaired plasmid was isolated from His^+ colonies. The *gcs1-R54A* plasmid was generated with a QuikChange Site-Directed Mutagenesis Kit (Stratagene, La Jolla, CA) using pRS313-GCS1 as a template. The entire open reading frame of *GCS1* was sequenced to confirm that only the desired mutation was introduced. The plasmids used in this study are listed in Table II. Schemes detailing the construction of all the plasmids are available on request. The appropriate references for GFP-Snc1p, GFP-Rer1p, Chs3p-GFP and mRFP1-Snc1p are listed in the right column of Table II. GFP-Tlg1p was functional, because YEplac181-GFP-TLG1 rescued the lethality of *tlg1Δ* mutant in the YEF473 strain background (our unpublished results).

Microscopic Observations

Cells were observed with a Nikon ECLIPSE E800 microscope equipped with an HB-10103AF super high-pressure mercury lamp and a 1.4 NA 100x Plan Apo oil immersion objective lens with the appropriate fluorescence filter sets or differential interference contrast optics (Nikon Instec, Tokyo, Japan). Images were acquired with a digital cooled CCD camera (C4742-95-12NR; Hamamatsu photonics K.K., Hamamatsu, Japan) using the AQUACOSMOS software package (Hamamatsu photonics). Observations are based on the examination of at least 100 cells.

To visualize GFP- or mRFP1-tagged proteins in living cells, cells were grown in YPDA, harvested, and resuspended in SD medium. Cells were mounted on a glass microslide, followed by immediate observation using a GFP bandpass or G-2A filter set. When the effect of latrunculin A (LAT-A, Wako Pure Chemicals, Osaka, Japan) was examined, cells were treated with 100 μM LAT-A by the addition of a 20 mM stock solution in dimethyl sulfoxide (DMSO) to the medium as described previously (Ayscough *et al.*, 1997).

Staining with the lypophilic stylyl dye FM4-64 (*N*-(3-triethylammoniumpropyl)-4-(*p*-diethylaminophenylhexatrienyl) pyridinium dibromide) was performed as described previously with minor modifications (Misu *et al.*, 2003). Briefly, cells were grown in YPDA at 30°C for 6.5 h. Four OD_{600} units of cells were collected by centrifugation, suspended in 100 μl of YPDA, and labeled in 32 μM FM4-64 (Molecular Probes, Eugene, OR) for 30 min on ice. Cells were harvested by centrifugation, resuspended in 200 μl of fresh YPDA, and chased at 30°C for the indicated time periods. After the chase, cells were washed with SD medium, followed by immediate microscopic observation using a G-2A filter set. The vacuole lumen was visualized using CellTracker Blue CMAC (Molecular Probes) according to the manufacturer's protocol.

Cell Labeling and Immunoprecipitation

Vacuolar sorting of carboxypeptidase Y (CPY) was examined by pulse-chase analysis and immunoprecipitation experiments as described previously with minor modifications (Misu *et al.*, 2003; Rothblatt and Schekman, 1989). Briefly, cells were grown in low-sulfate SD medium at 30°C for 7.5 h, washed, resuspended in sulfate-free SD medium, and grown at 30°C for 30 min. Cells were labeled with 50 μCi of Trans^{35}S-label

(ICN Radiochemicals, Irvine, CA) for 10 min before they were chased for the indicated time periods. CPY was immunoprecipitated with rabbit antibodies against CPY (a gift from Y. Ohsumi, National Institute for Basic Biology, Okazaki, Japan), resolved by SDS-PAGE, and visualized with a phosphorimager system (Fuji Photo Film, Tokyo, Japan).

Secretion of invertase was also examined by pulse-chase analysis and immunoprecipitation experiments as described previously with minor modifications (Rothblatt and Schekman, 1989). Briefly, cells were grown in low-sulfate SD medium containing 5% glucose at 30°C for 7.5 h. Cells were then converted to spheroplasts with zymolyase, transferred to sulfate-free SD medium containing 0.1% glucose, and further grown at 30°C for 30 min to induce invertase expression. Cells were labeled with 50 μCi of Trans^{35}S-label at 30°C for 4 min before they were chased. To terminate the chase, NaN_3 was added to a final concentration of 10 mM. Cell suspensions were separated into spheroplasts and media by centrifugation to obtain intracellular and extracellular fractions, respectively. Intracellular and extracellular fractions were immunoprecipitated with anti-invertase antisera (a gift from A. Nakano, The University of Tokyo, Japan). The immunoprecipitated invertase was resolved by SDS-PAGE, and visualized using a phosphorimager system.

Electron Microscopy (EM)

Ultrastructural observation of cells by conventional EM was performed using the glutaraldehyde-osmium fixation technique as described previously (Wright, 2000; Banta *et al.*, 1988). Briefly, cells were fixed in 2% glutaraldehyde, treated for 10 min in 1% sodium metaperiodate, and postfixed in 2% reduced osmium. Cells were then embedded in Q651 resin (Nissin EM, Tokyo, Japan). Thin sections (50-60 nm) were cut on

an Ultracut microtome (Leica, Wetzlar, Germany) equipped with a Sumiknife (Sumitomo Electric Industries, Osaka, Japan), stained with 3% uranyl acetate and Reynold's lead citrate, and viewed using an H-7100 electron microscope (HITACHI, Tokyo, Japan) at 75 kV. Immuno-EM was performed using the aldehyde fixation/metaperiodate permeabilization method as described previously (Mulholland and Botstein, 2002), except glutaraldehyde was not included in the fixative. Cells were embedded in LR White resin (medium grade; London Resin Company, Berkshire, UK), and sectioned as described above. Mouse anti-HA antibodies (HA.11; BAbCO, Richmond, CA) were used as primary antibodies at a 1:500 dilution. Ten-nm gold-conjugated anti-mouse IgG antibodies (BBInternational, Cardiff, UK) were preadsorbed with fixed wild-type cells, and used as secondary antibodies at a 1:100 dilution. Samples were poststained with uranyl acetate and viewed as described above.

Results

Arf1p and Arf2p are Involved in the Endocytic Recycling Pathway

In accord with the previous study that identified *DRS2* in a genetic screen for mutations that are synthetically lethal with the *arf1Δ* mutation (Chen *et al.*, 1999), the *arf1Δ* mutant displayed a growth defect when Cdc50p was depleted by using the P_{GAL1}*-3HA-CDC50* allele, which employs the glucose-repressible *GAL1* promoter to control the expression of Cdc50p (Fig. 1A). This synthetic genetic interaction with *arf1Δ* was specific, and was not observed with mutations in other genes encoding Arf and Arf-like proteins, including *ARF2*, *ARF3*, *ARL1*, and *ARL3* (Fig. 2A). Several *arf1*-ts *arf2Δ* mutants were isolated and some of these mutations appeared to show synthetic lethality with *drs2Δ* (Yahara *et al.*, 2001). Interestingly, the *arf1-18 arf2Δ* mutant, which did not exhibit impaired Golgi-to-ER transport, exocytosis, or endocytic

transport to vacuoles at the restrictive temperature (Yahara *et al*., 2001), displayed a growth defect when Cdc50p was depleted (Fig. 1A). These results suggest that Arf and Cdc50p-Drs2p functionally overlap in a vesicular transport pathway that is distinct from those described above.

We previously demonstrated the involvement of Cdc50p-Drs2p in endocytic recycling of GFP-Snc1p (Saito *et al*., 2004). Snc1p is an exocytic v-SNARE that normally cycles from the plasma membrane through the early endosome to the TGN and back to the plasma membrane (Lewis *et al*., 2000). We examined the localization of GFP-Snc1p in the *arf1Δ* and *arf1-18 arf2Δ* mutants. At the permissive temperature (30°C), GFP-Snc1p was primarily localized to the plasma membrane, and was concentrated within polarized growth sites such as buds or cell division sites in the *arf1-18 arf2Δ* mutant, as well as in the wild-type strain (Fig. 1B). At the restrictive temperature (37°C), however, GFP-Snc1p was diffusely distributed in the cytoplasm or accumulated as small punctate structures in the *arf1-18 arf2Δ* mutant. In the *arf1Δ* mutant, 58% (n=103) and 70% of the cells (n=102) accumulated GFP-Snc1p in intracellular structures at 30°C and 37°C, respectively (Fig. 1B). In addition, GFP-Snc1p was also localized to ring structures in 24% (n=103) and 21% of the cells (n=103) at 30°C and 37°C, respectively (Fig. 1B, arrowhead). In contrast, GFP-Snc1p (pm), an endocytosis-defective mutant form of Snc1p (Lewis *et al*., 2000), was exclusively localized to the plasma membrane in the *arf1-18 arf2Δ* mutant at the restrictive temperature and in the *arf1Δ* mutant, as well as in the wild-type strain (Fig. 1B). These data indicate that the intracellular accumulation of Snc1p-containing structures in the *arf1* mutants was not caused by defects in the exocytotic pathway from the TGN to the plasma membrane, but was dependent on endocytosis. The TGN marker Sec7p-mRFP1 (Robinson *et al*., 2006) was localized to internal punctate structures in the *arf1-18 arf2Δ* and *arf1Δ* mu-

tants as it was in wild-type cells, suggesting that the Snc1p-containing structures were not derived from the TGN (Fig. 1C). These results suggest that Arf1p and Arf2p are involved in the regulation of the endocytic recycling pathway.

CDC50 Exhibits a Specific Genetic Interaction with GCS1 among ARF GAP Genes

Because Arf1p and Arf2p seem to be involved in multiple vesicle transport pathways, dissection of the defects in the *arf1 cdc50Δ* mutant may be difficult. Therefore, we investigated the genetic interaction between *CDC50* and genes encoding regulators of Arf proteins (Arf GAPs and Arf GEFs). The *cdc50Δ* mutant was crossed with a null mutant or a ts mutant of the Arf regulators and the growth of double or triple mutants was examined using tetrad analysis (Fig. 2A). Single mutations in the Arf GEF genes (*sec7-1*, *syt1Δ*, *gea1Δ*, and *gea2Δ*) or the *gea1*-ts *gea2Δ* mutations (*gea1-4 gea2Δ*, *gea1-6 gea2Δ*, and *gea1-19 gea2Δ*) did not affect the growth of the *cdc50Δ* mutant at 30°C. Interestingly, among the mutations in the genes coding for Arf GAPs (*gcs1Δ*, *glo3Δ*, *age1Δ*, and *age2Δ*), the *gcs1Δ* mutation displayed synthetic lethality with the *cdc50Δ* mutation (Fig. 2B). The *drs2Δ* mutation exhibited the same genetic interaction pattern with the mutations in the genes coding for Arf GAPs (our unpublished results). Consistent with our results, Robinson *et al*. (2006) recently identified the synthetic lethal interaction between *drs2Δ* and *gcs1Δ* by synthetic genetic analysis. The Arf GAP activity-defective *gcs1-R54A* mutation (Yanagisawa *et al*., 2002) failed to rescue the Cdc50p-depleted *gcs1Δ* mutant from lethality (Fig. 2D), suggesting that the Gcs1p-mediated regulation of Arf1p was required for growth of the Cdc50p-depleted wild-type cells. We therefore decided to examine the defects in the vesicular transport pathways in the Cdc50p-depleted *gcs1Δ* mutant.

The Endocytic, Exocytotic, and CPY Transport Pathways are not Impaired in the Cdc50p-depleted gcs1Δ Mutant

To investigate essential functions governed by Gcs1p and Cdc50p-Drs2p, we constructed the P_{GAL1}*-3HA-CDC50 gcs1Δ* mutant. As shown in Fig. 2C, the P_{GAL1}*-3HA-CDC50 gcs1Δ* mutant grew normally in the galactose-containing medium, but not in the glucose-containing medium. After 3-h incubation in the glucose-containing medium, the expression of 3HA-Cdc50p was not detected in the immunoblot analysis either by the anti-3HA or -Cdc50p antibodies (our unpublished results). Because complete growth arrest required incubation for at least 6 h in the glucose-containing medium (our unpublished results), the phenotypes of the P_{GAL1}*-3HA-CDC50 gcs1Δ* mutant (the P_{GAL1}*-3HA-CDC50* allele is hereafter referred to as Cdc50p-depleted) were analyzed after incubation for more than 6 h at 30°C.

Endocytic internalization and transport to vacuoles was examined in the Cdc50p-depleted *gcs1Δ* mutant at 30°C with the fluorescent endocytic marker FM4-64. Cells were depleted of Cdc50p for 6.5 h, labeled with FM4-64, and chased. As in the wild-type cells, FM4-64 was internalized and delivered to vacuoles after a 1-h chase in the Cdc50p-depleted *gcs1Δ* mutant (Fig. 3A). These results also revealed that the vacuoles in the Cdc50p-depleted *gcs1Δ* mutant were somewhat fragmented. The endocytic marker Lucifer Yellow and the α-factor receptor Ste2p-GFP were similarly delivered to vacuoles in the Cdc50p-depleted *gcs1Δ* mutant (our unpublished results). These results indicate that endocytosis was not severely impaired in the Cdc50p-depleted *gcs1Δ* mutant.

The vacuolar protein sorting pathway was assessed in the Cdc50p-depleted *gcs1Δ* mutant by monitoring the maturation of the soluble vacuolar protein CPY. Pulse-chase experiments were performed after depletion of Cdc50p for 8 h in glu-

cose-containing medium. During transport of CPY from the ER through the TGN to vacuoles, CPY undergoes a series of characteristic modifications. CPY is found as a 67-kDa precursor species (P1) and a fully glycosylated 69-kDa precursor form (P2) in the ER and the Golgi, respectively. It was previously reported that the kinetics of the maturation of CPY were delayed in the *drs2Δ*, *cdc50Δ*, and *dnf1Δ drs2Δ* mutants at lower temperatures (Misu *et al*., 2003; Hua *et al*., 2002; Chen *et al*., 1999). The conversion of CPY from P1 through P2 to the mature form (m), however, was completed in 15 min at 30°C in the Cdc50p-depleted wild-type cells, as well as in the wild-type strain and the *gcs1Δ* mutant (Fig. 3B). Although the Cdc50p-depleted *gcs1Δ* mutant accumulated a small amount of the P2 form, most of the CPY was converted to the mature form during the 30-min chase. Because defects in vacuolar protein sorting lead to secretion of CPY, we also examined CPY sorting by colony immunoblotting. Although CPY was secreted from the *vps1Δ* cells, it was not secreted from the Cdc50p-depleted *gcs1Δ*, Cdc50p-depleted wild-type, and *gcs1Δ* cells (our unpublished results). These results suggest that CPY transport was not severely impaired in the Cdc50p-depleted *gcs1Δ* mutant.

To investigate the secretory pathway in the Cdc50p-depleted *gcs1Δ* mutant, we examined the processing and secretion of the periplasmic enzyme invertase in pulse-chase experiments using P_{GAL1}*-3HA-CDC50 gcs1Δ* cells that were depleted of Cdc50p for 8 h. After a 60-min chase, invertase was processed to a highly glycosylated form, which was predominantly found in the extracellular fraction in the experiments with the Cdc50p-depleted *gcs1Δ* strain, as well as in the experiments with the wild-type, Cdc50p-depleted wild-type, and *gcs1Δ* cells (Fig. 3C). These data suggest that the secretory pathway was not severely impaired in the Cdc50p-depleted *gcs1Δ* mutant.

To investigate the Golgi-to-ER retrograde transport pathway, we observed the localization of GFP-Rer1p in the Cdc50p-depleted *gcs1Δ* mutant. Rer1p is a membrane protein found in the cis-Golgi that serves as a retrieval receptor for ER-resident membrane proteins (Sato *et al*., 1997, 2001). It has been shown that when the Golgi-to-ER retrograde transport is blocked by impairment in the COPI-dependent pathway, the majority of GFP-Rer1p is transported to vacuoles (Sato *et al*., 2001). GFP-Rer1p was localized to internal punctate structures in the Cdc50p-depleted *gcs1Δ* mutant and control strains in a manner that resembled Golgi localization (Fig. 3D). These data suggest that the Golgi-to-ER retrograde transport was not impaired in the Cdc50p-depleted *gcs1Δ* mutant.

Taken together, our results suggest that the Cdc50p-depleted *gcs1Δ* mutant was defective in a more selective vesicle transport pathway. This is in contrast to previous observations that the Arf GAPs Gcs1p and Age2p provide essential functions for transport from the TGN (Poon *et al*., 2001), and that Gcs1p and Glo3p are required for retrograde transport from the Golgi to the ER (Poon *et al*., 1999). In the Cdc50p-depleted *gcs1Δ* mutant, it seems that Age2p and Glo3p compensated for these essential functions.

The Late Endosome-to-TGN Retrieval Pathway is not Impaired in the Cdc50p-depleted gcs1Δ Mutant

To investigate the retrieval pathway from late endosomes to the TGN in the Cdc50p-depleted *gcs1Δ* mutant, we examined the localization of two TGN resident membrane proteins, Kex2p and Vps10p, whose TGN localization is dependent on the late endosome-to-TGN retrieval pathway. Kex2p is required for maturation of the precursors of secreted peptides and proteins, including the α-mating factor (Fuller *et al*., 1988; Julius *et al*., 1984). Vps10p is a CPY sorting receptor, which dissociates from

its cargo at the late endosome (Cooper and Stevens, 1996; Marcusson *et al*., 1994). Kex2p and Vps10p are recycled back from late endosomes to the TGN in a retromer-dependent manner (Seaman *et al*., 1998), whereas Kex2p is also transported to early endosomes and retrieved to the TGN by an unknown mechanism (Lewis *et al*., 2000).

Vps10p-GFP localized to punctate structures in the wild-type strain (Fig. 4A), whereas deletion of *VPS26*, a component of retromer, caused mislocalization of Vps10p-GFP to vacuoles as assessed by staining with CMAC (our unpublished results), suggesting that Vps10p-GFP is normally retrieved from late endosomes to the TGN by the retromer-dependent mechanism. The localization of Vps10p-GFP to internal punctate structures was normal in the Cdc50p-depleted *gcs1Δ* mutant (Fig. 4A). Kex2p-GFP localizes to punctate structures that appeared to be endosomes or TGN compartments in the wild-type strain (Chen *et al*., 2005), and it was not localized to vacuoles as assessed by staining with CellTracker Blue CMAC (Fig. 4B). In the Cdc50p-depleted wild-type and the *gcs1Δ* cells, Kex2p-GFP was also localized to punctate structures, although a fraction was mislocalized to vacuoles (Fig. 4A). In contrast, in the Cdc50p-depleted *gcs1Δ* mutant, Kex2p-GFP was almost mislocalized to the vacuolar compartments (Fig. 4, A and B). Proteins such as Kex2p and Vps10p that cycle via endosomes are mislocalized to the vacuole if their cycling is impaired (Conibear and Stevens, 2000; Cooper and Stevens, 1996; Wilcox *et al*., 1992). Our results imply that the Cdc50p-depleted *gcs1Δ* mutant was defective in the early endosome-to-TGN transport pathway, but not in the late endosome-to-TGN transport pathway.

The Cdc50p-depleted gcs1Δ Mutant is Defective in the Retrieval Pathway from Early

Endosomes to the TGN

Defective retrieval of Kex2p from early endosomes in the Cdc50p-depleted *gcs1Δ* mutant is consistent with the results that *arf1* mutants are defective in endocytic recycling of GFP-Snc1p (Fig. 1B). Thus, we investigated defects in the early endosome-to-TGN transport pathway in the Cdc50p-depleted *gcs1Δ* mutant. Robinson *et al*. (2006) reported that the *gcs1Δ* mutant accumulated GFP-Snc1p in intracellular compartments. In our *gcs1Δ* mutant derived from the YEF473 strain, such mislocalization of GFP-Snc1p was observed at 18°C (our unpublished results), whereas at 30°C GFP-Snc1p was primarily localized to the plasma membrane at polarized sites, and some of the protein were localized to internal punctate structures that appeared to be early endosomes or TGN compartments (Fig. 5A), as in the wild-type strain (Lewis *et al*., 2000). In 80% of the P_{GAL1}*-3HA-CDC50* mutant cells depleted of Cdc50p for 8 h at 30°C, the localization pattern of GFP-Snc1p was indistinguishable from that in wild-type cells, whereas in the remaining 20% of the cells, GFP-Snc1p was not localized to the plasma membrane and instead accumulated in intracellular structures (n = 113) (Fig. 5A and our unpublished results). In 99% of the Cdc50p-depleted *gcs1Δ* mutant cells (n = 104), however, GFP-Snc1p was not observed on the plasma membrane, and instead accumulated in aberrant membrane structures (Fig. 5A). These GFP-Snc1p-positive structures in the Cdc50p-depleted *gcs1Δ* mutant were distinct from vacuoles that were visualized by staining with CMAC (our unpublished results). The accumulation of GFP-Snc1p in aberrant membrane structures in the Cdc50p-depleted *gcs1Δ* mutant was observed even after 3-h incubation to deplete Cdc50p, suggesting that mislocalization of GFP-Snc1p in this mutant reflected primary defects caused by depletion of Cdc50p in the *gcs1Δ* mutant (our unpublished results).

The localization of GFP-Snc1p to the plasma membrane was somewhat re-

stored, when the Cdc50p-depleted *gcs1Δ* mutant cells were treated with LAT-A for 1 h, which sequesters actin monomers and thereby inhibits endocytosis, after 7-h incubation to deplete Cdc50p (Fig. 5B, arrowhead). These results suggest that GFP-Snc1p is delivered to the plasma membrane and then is endocytosed before accumulating in the intracellular structures in the Cdc50p-depleted *gcs1Δ* mutant. In the Cdc50p-depleted wild-type and the *gcs1Δ* cells, GFP-Snc1p was exclusively localized to the plasma membrane after the treatment with LAT-A for 1 h as in the wild-type strain (our unpublished results). Thus, endocytic recycling of GFP-Snc1p is slowed, but not blocked in the Cdc50p-depleted wild-type cells. In contrast, the intracellular GFP-Snc1p-containing structures were still observed in the Cdc50p-depleted *gcs1Δ* mutant, suggesting the severe impairment of endocytic recycling in this mutant.

Chs3p, a subunit of the cell wall biosynthetic enzyme chitin synthase III, is localized to the plasma membrane at mother-bud junctions and in punctate intracellular structures (Valdivia *et al*., 2002; Santos and Snyder, 1997; Chuang and Schekman, 1996; Ziman *et al*., 1996). Similar to Snc1p, this protein is thought to be transported through the endocytic recycling pathway (Lewis *et al*., 2000; Holthuis *et al*., 1998b). Thus, we observed the localization of Chs3p-GFP in Cdc50p-depleted *gcs1Δ* mutant cells that simultaneously expressed mRFP1-Snc1p (Robinson *et al*. 2006). In the Cdc50p-depleted wild-type, the *gcs1Δ*, and the wild-type cells, Chs3p-GFP was primarily localized to intracellular punctate structures that presumably corresponding to early endosomes or TGN compartments, and some of these structures colocalized with mRFP1-Snc1p (Fig. 6A). Only 3% of the Cdc50p-depleted wild-type cells (n = 101) and 1% of the *gcs1Δ* cells (n = 100) exhibited the accumulation of Chs3p-GFP in aberrant membrane structures. In contrast, in 96% of the Cdc50p-depleted *gcs1Δ* cells (n = 103), Chs3p-GFP accumulated in aberrant membrane structures, which largely colocal-

ized with mRFP1-Snc1p.

We also observed the localization of Tlg1p, a member of the syntaxin family of t-SNAREs that is recycled between early endosomes and the TGN (Lewis *et al*., 2000; Holthuis *et al*., 1998a), in Cdc50p-depleted *gcs1Δ* mutant cells that simultaneously expressed mRFP1-Snc1p. Similar to Chs3p-GFP, in 99% of the Cdc50p-depleted wild-type cells (n = 115) and 99% of the *gcs1Δ* single mutant (n = 100), GFP-Tlg1p was localized to intracellular punctate structures as in the wild-type strain (Fig. 6B). In 99% of the Cdc50p-depleted *gcs1Δ* mutant cells (n = 103), however, aberrant membrane structures containing both GFP-Tlg1p and mRFP1-Snc1p were observed. These results suggest that Chs3p-GFP, GFP-Tlg1p, and mRFP1-Snc1p accumulated in the same membrane structures in the Cdc50p-depleted *gcs1Δ* mutant.

To examine whether the aberrant membrane structures seen in the Cdc50p-depleted *gcs1Δ* mutant were TGN compartments, we observed the localization of Sec7p-mRFP1, and compared it with that of GFP-Tlg1p. Consistent with the previous data that Tlg1p is localized to early endosomes and the TGN (Lewis *et al*., 2000; Holthuis *et al*., 1998b), GFP-Tlg1p partially colocalized with Sec7p-mRFP1 in the wild-type, Cdc50p-depleted wild-type, and *gcs1Δ* cells (Fig. 6C). In the Cdc50p-depleted *gcs1Δ* mutant, Sec7p-mRFP1 gave a similar punctate pattern, and did not colocalize with GFP-Tlg1p, suggesting that the GFP-Tlg1p-containing structures were independent of the TGN membranes.

Taken together, our results suggest that the Cdc50p-depleted *gcs1Δ* mutant was defective in the retrieval pathway from early endosomes to the TGN, and that GFP-Snc1p, GFP-Tlg1p, and Chs3p-GFP all accumulated in the same aberrant endosomal structures.

Gga1p and Gga2p are Required for Growth and the Early Endosome-to-TGN Transport in the Cdc50p-depleted wild-type cells

We next investigated genetic interactions between *cdc50Δ* and mutations in genes coding for proteins that have been implicated in Arf1-mediated or clathrin-coated vesicle budding. These include GGAs (*gga1Δ* and *gga2Δ*) (Costaguta *et al*., 2001; Dell'Angelica *et al*., 2000; Hirst *et al*., 2000), clathrin (*chc1-521*) (Chen and Graham, 1998), clathrin-associated AP complexes (*apl2Δ*, *apl4Δ*, *apm1Δ*, and *aps1Δ* for AP-1 and *apl5Δ*, *apl6Δ*, *apm3Δ*, and *aps3Δ* for AP-3) (Yeung *et al*., 1999), and COPI (*sec21-1*) (reviewed in Kreis *et al*., 1995; Letourneur *et al*., 1994). The *cdc50Δ* mutant was crossed with the respective mutants and the growth of double or triple mutants was examined using tetrad analysis (Fig. 7A). Consistent with previous observations with the *drs2Δ* mutation (Chen *et al*., 1999), the *cdc50Δ* mutation exhibited synthetic growth defects with the *chc1-521* mutation, but not with the *sec21-1* mutation. Interestingly, the *gga1Δ gga2Δ* mutation exhibited synthetic lethality with the *cdc50Δ* mutation. To examine the effects of the *gga1Δ* or *gga2Δ* single mutation on the growth of the *cdc50Δ* mutant more precisely, we constructed P_{GAL1}*-3HA-CDC50 ggaΔ* mutants in the S288C background in which mutations in GGAs, AP-1, and AP-3 in Fig. 7A were constructed. It was previously reported that the *gga2Δ* mutation, but not the *gga1Δ* mutation, exhibited synthetic growth defects in combination with the deletion of *APL2* (the gene encoding the β1 subunit of AP-1) or the *chc1-521* mutation (Costaguta *et al*., 2001), suggesting that the Gga2p is the major Gga protein. Consistently, the Cdc50p-depleted *gga2Δ* mutant exhibited the slow growth, whereas the Cdc50p-depleted *gga1Δ* mutant grew normally (Fig. 7B).

Because Gga1p and Gga2p are involved in the TGN-to-late endosome transport of CPY (Zhdankina *et al*., 2001; Dell'Angelica *et al*., 2000; Hirst *et al*., 2000), we ex-

amined the mutants after an 8-h culture at 30°C to determine whether the depletion of Cdc50p affect the CPY sorting in the *gga* mutants. The maturation of CPY was normal in the *gga1Δ*, *gga2Δ*, Cdc50p-depleted wild-type, and Cdc50p-depleted *gga1Δ* cells as well as in the wild-type strain (Fig. 7C and our unpublished results), whereas the Cdc50p-depleted *gga2Δ* mutant exhibited a slight delay in the maturation. Additionally, a small amount of the P2 form of CPY accumulated in the *gga1Δ gga2Δ* mutant as described previously (Zhdankina *et al*., 2001; Dell'Angelica *et al*., 2000; Hirst *et al*., 2000), and the depletion of Cdc50p slightly exacerbated this phenotype (Fig. 7C). Although about 50% of CPY matured within 15 min, the depletion of Cdc50p slightly exacerbated this phenotype (Fig. 7C), indicating that the CPY transport pathway was impaired in the Cdc50p-depleted *gga1Δ gga2Δ* mutant.

To examine the endocytic recycling pathway in the Cdc50p-depleted *ggaΔ* mutants, we observed the localization of mRFP1-Snc1p and GFP-Tlg1p in these cells. mRFP1-Snc1p was primarily localized to the plasma membrane at polarized growth sites in the *gga1Δ*, *gga2Δ*, and Cdc50p-depleted *gga1Δ* mutants, as well as in the wild-type strain (Fig. 8 and our unpublished results). Consistent with a previous report (Black and Pelham, 2000), mRFP1-Snc1p was primarily localized to intracellular punctate structures in 81% of the *gga1Δ gga2Δ* cells (n = 103). The defects in the endocytic recycling pathway in the *gga1Δ gga2Δ* mutant, however, seemed to be mild, because GFP-Tlg1p exhibited a normal punctate localization and partial colocalization with mRFP1-Snc1p in the mutant cells, as was observed in the *gga1Δ*, *gga2Δ*, Cdc50p-depleted *gga1Δ*, and wild-type strains (Fig. 8 and our unpublished results). In contrast, mRFP1-Snc1p and GFP-Tlg1p accumulated in aberrant membrane structures in most of the Cdc50p-depleted *gga2Δ* and Cdc50p-depleted *gga1Δ gga2Δ* mutant cells, as was observed with the Cdc50p-depleted *gcs1Δ* mutant, suggesting that the retrieval

pathway from early endosomes to the TGN was severely impaired in these mutants. When these cells were treated with LAT-A at 30°C for 1 h after a 7-h incubation to deplete the cell of Cdc50p, the plasma membrane localization of GFP-Snc1p was observed in the *gga1Δ gga2Δ*, Cdc50p-depleted *gga2Δ*, and Cdc50p-depleted *gga1Δ gga2Δ* mutants (our unpublished results), suggesting that the accumulation of the aberrant Snc1p-containing structures was dependent on endocytosis. These data also imply that the late secretory pathway was not severely impaired in the Cdc50p-depleted *ggaΔ* mutants.

Taken together, these data suggest that like the Cdc50p-depleted *gcs1Δ* mutant, the Cdc50p-depleted *gga1Δ gga2Δ* mutant was defective in the retrieval pathway from early endosomes to the TGN.

Localization of AP-1 to Endosomal/TGN Membranes Requires Cdc50p and Gcs1p

Because AP-1 and COPI have been implicated in the retrieval pathway from early endosomes to the TGN (Robinson *et al*., 2006; Cai *et al*., 2005; Valdivia *et al*., 2002; Lewis *et al*., 2000), we further examined genetic interactions between *CDC50* or *GCS1* and two genes encoding coat proteins. Interestingly, the *apl2Δ* mutation, but not the *sec21-1* mutation (γ subunit of COPI), caused mild growth defects with the *gcs1Δ* mutation (Fig. 9A and our unpublished results), whereas the *cdc50Δ* mutation did not exhibit genetic interaction with these genes (Fig. 7A). This growth defect may be caused by defective early endosome-to-TGN transport: the *apl2Δ* and *gcs1Δ* mutants displayed a normal localization of GFP-Snc1p, whereas GFP-Snc1p accumulated in intracellular membrane structures of 79% of the *apl2Δ gcs1Δ* cells (n = 105; Fig. 9B). These results are consistent with the idea that AP-1 is involved in the formation of CCVs from early endosomes (Valdivia *et al*., 2002). To examine whether AP-1 is localized to

early endosomes, we constructed strains expressing the integrated version of *APL4-GFP* (the gene encoding the γ subunit of AP-1), as a sole copy of *APL4*. The *APL4-GFP* allele was functional, as assessed by the growth phenotype of the mutant with *APL4-GFP* in combination with the *gga1Δ gga2Δ* mutation, which causes synthetic growth defects with the *apl4Δ* mutation at the restrictive temperature (Costaguta *et al*., 2002 and our unpublished results). Apl4p-GFP was localized to internal punctate structures in the wild-type strain, in a manner that resembled endosomal/TGN compartments (Fig. 9C). Microscopic examination of wild-type cells co-expressing Apl4p-GFP and Sec7p-mRFP1 revealed that Apl4p-GFP partially colocalized with Sec7p-mRFP1 (Fig. 9C). Interestingly, 32% of the Apl4p-GFP-containing punctate structures (69 of the 217 puncta in 55 cells) did not colocalize with Sec7p-mRFP1 (Fig. 9C, arrowhead), suggesting that Apl4p-GFP was also localized to endosomal compartments. The early endosome could be visualized after brief incubation with FM4-64 (Vida and Emr, 1995). Wild-type cells expressing Apl4p-GFP were labeled with FM4-64 at 0°C, incubated for 3 min at 30°C, and immediately observed by fluorescence microscopy. Thirty-two % of the Apl4p-GFP-containing structures (27 of the 84 puncta in 18 cells) were labeled with FM4-64 (Fig. 9D, arrowhead). These results suggest that AP-1 localizes to both early endosomes and the TGN. Localization of AP-1 to endosomal membranes and defects in the early endosome-to-TGN transport pathway in the Cdc50p-depleted *gcs1Δ* mutant prompted us to examine the localization of Apl4p-GFP in the Cdc50p-depleted *gcs1Δ* mutant. Apl4p-GFP was localized to intracellular punctate structures in the *cdc50Δ* and *gcs1Δ* mutants as well as in the wild-type strain (Fig. 9E). In contrast, in the Cdc50p-depleted *gcs1Δ* mutant cells, Apl4p-GFP was observed in a hazy pattern distributed throughout the cell, in addition to some punctate structures (Fig. 9E). These results suggest that Cdc50p and Gcs1p have

redundant functions in the recruitment of AP-1 to endosomal/TGN membranes, and that defects in the early endosome-to-TGN transport in the Cdc50p-depleted *gcs1Δ* mutant may be partly due to a failure in the recruitment of AP-1 to early endosome membranes.

The Cdc50p-depleted gcs1Δ Mutant Accumulates Abnormal Membrane Structures

EM has previously revealed the accumulation of large abnormal double-membrane structures with crescent- or ring-shaped morphologies in the *cdc50Δ* and *drs2Δ* mutants grown at lower temperatures (Misu *et al*., 2003; Chen *et al*., 1999; our unpublished results) and in the Cdc50p-depleted *erg3Δ* mutant growth at 30°C (Kishimoto *et al*., 2005). When grown in YPDA medium at 30°C for 8 h to deplete the cells of Cdc50p, the P_{GAL1}*-3HA-CDC50 gcs1Δ* mutant cells accumulated a large number of similar structures [12.5 abnormal membrane structures (>200 nm in diameter)/10 μm^2, n = 32 sections]. In contrast, the P_{GAL1}*-3HA-CDC50* mutant cells accumulated a little (2.3 structures/10 μm^2, n = 30 sections), and the *gcs1Δ* mutant cells did not (Fig. 10A). To examine whether these abnormal structures were the same as the Snc1p-containing structures shown in Fig. 5A, we performed immuno-EM on Cdc50p-depleted *gcs1Δ* cells expressing 3HA-tagged Snc1p (Robinson *et al*. 2006). As shown in Fig. 10B, the abnormal double-membrane structures were labeled with immunogold particles in the Cdc50p-depleted *gcs1Δ* mutant, but not in control Cdc50p-depleted *gcs1Δ* cells expressing untagged Snc1p (our unpublished results).

The Cdc50p-depleted *gga1Δ gga2Δ* and *apl2Δ gcs1Δ* mutants were also examined for the accumulation of abnormal membrane structures by EM. When the cells were depleted of Cdc50p for 8 h, crescent- or ring-shaped membrane structures accumulated in the Cdc50p-depleted *gga2Δ* and Cdc50p-depleted *gga1Δ gga2Δ* mutant cells, as was observed in the Cdc50p-depleted *gcs1Δ* mutant, whereas these structures were

rarely observed in the *gga1Δ*, *gga2Δ*, and *gga1Δ gga2Δ* mutant cells (Fig. 11A and our unpublished results). Crescent- or ring-shaped membrane structures also accumulated in the *apl2Δ gcs1Δ* mutant cells, although this phenotype was mild; abnormal membrane structures (>200 nm in diameter) were fewer (1.5 structures/10 μm^2, n = 32 sections) compared with the Cdc50p-depleted *gcs1Δ* mutant (12.5 structures/10 μm^2, n = 32 sections) and the Cdc50p-depleted *gga1Δ gga2Δ* mutant (5.7 structures/10 μm^2, n = 30 sections) (Fig. 11B and our unpublished results). Thus, it seems that the severity of the growth defect in these mutants is correlated with the extent to which abnormal membranes are intracellularly accumulated.

Taken together with the results obtained by fluorescence microscopy, these results imply that the Cdc50p-depleted *gcs1Δ*, Cdc50p-depleted *gga1Δ gga2Δ*, and *apl2Δ gcs1Δ* mutants are defective in the formation of vesicles destined for the TGN from early endosomes.

Discussion

The Cdc50p-Drs2p Putative APLT is Involved in the Arf-mediated Retrieval Pathway from Early Endosomes to the TGN

It was previously suggested that Drs2p is involved in Arf1p- and clathrin-dependent vesicle formation; *DRS2* was identified as a synthetic-lethal mutation with *arf1Δ* (Chen *et al*., 1999; Chen and Graham, 1998), and fewer CCVs were isolated from *drs2Δ* cells than from wild-type cells (Chen *et al*., 1999). Some of these CCVs may have been post-Golgi secretory vesicles, because the *drs2Δ* mutation reduced the number of vesicles that accumulated when the actin cytoskeleton was disrupted (Gall *et al*., 2002). On the other hand, the involvement of Arf1p and Arf2p in the endocytic pathways has been suggested (Yahara *et al*., 2001; Gaynor *et al*., 1998). The effects of the *cdc50Δ*

and *drs2Δ* mutations on the formation of endocytic vesicles, however, cannot be assessed by disruption of the actin cytoskeleton, because endocytosis is dependent on the actin cytoskeleton in yeast (Engqvist-Goldstein and Drubin, 2003). Snc1p-containing membrane structures accumulated in the *arf1Δ* and *arf1-18 arf2Δ* mutants in an endocytosis-dependent manner. Ultrastructural analyses revealed that the *arf1Δ* and some *arf1*-ts *arf2Δ* mutants contained unusual membranous structures, such as discontinuous ring-like or Golgi stack-like structures (Yahara *et al*., 2001; Gaynor *et al*., 1998), which may have been derived from endosomes. Thus, the accumulation of abnormal structures in the Cdc50p-depleted *gcs1Δ* mutant that likely were a result of excessive early endosomal membranes may have been due to defective formation of CCVs or COPI vesicles (see below) from early endosomes. The involvement of clathrin in the endocytic recycling pathway has been demonstrated in mammalian cells (van Dam *et al*., 2002), and suggested in yeast; clathrin and AP-1 act to recycle Chs3p from early endosomes to the TGN (Valdivia *et al*., 2002). A mutant carrying the *chc1-521* allele, which is synthetically lethal with *cdc50Δ* or *drs2Δ* (Chen *et al*., 1999; our unpublished results), exhibited an intracellular accumulation of Snc1p, and this defect was exacerbated by depletion of Cdc50p (our unpublished results).

Because Arf1p is likely involved in multiple vesicular transport pathways (Yahara *et al*., 2001), the *cdc50 arf1* mutant should exhibit defects in various pathways, making the interpretation of the observed phenotypes complicated. To circumvent this problem, we explored genetic interactions between *CDC50* and regulators of *ARF1*, which are presumably involved in a more specific transport pathway. Gcs1p and Age2p provide overlapping essential function for transport from the TGN (Poon *et al*., 2001). Interestingly, the *cdc50Δ* mutation did not cause synthetic growth defects with the *age2Δ* mutation, suggesting that Gcs1p is specifically involved in the function of

Cdc50p-Drs2p. The Cdc50p-depleted *gcs1Δ* mutant did not exhibit apparent defects in post-Golgi vesicular transport pathways, presumably because Age2p compensates for the function of Gcs1p in these pathways. Recently, the Arf-like protein Arl1p was shown to be a potential substrate of Gcs1p (Liu *et al*., 2005), raising the possibility that the synthetic growth defect of the Cdc50p-depleted *gcs1Δ* mutant is caused by deregulation of Arl1p. The *arl1Δ* mutation, however, did not cause synthetic growth defects with the *cdc50Δ* mutation (our unpublished results). In addition, Arl1p has been implicated in vesicle fusion with TGN membranes (Panic *et al*., 2003), whereas we did not observe a discernible increase in the number of vesicles using EM sectioning of the Cdc50p-depleted *gcs1Δ* mutant (our unpublished results). Thus, it seems that the synthetic phenotypes in the Cdc50p-depleted *gcs1Δ* mutant are caused by deregulation of Arf1p.

In the current study, we have not identified a mutation in a gene encoding an Arf GEF that caused synthetic growth defects with the *cdc50Δ* mutation. It was previously reported that Drs2p physically interacts with Gea2p (Chantalat *et al*., 2004). GFP-Snc1p, however, was localized to the plasma membrane in the *gea1-4 gea2Δ* mutant even at the restrictive temperature (our unpublished results). Thus, this Drs2p-Gea2p interaction may play a specific role in the TGN function of Cdc50p-Drs2p as suggested previously (Chantalat *et al*., 2004).

Among the vesicular transport pathways examined in this study, only the retrieval pathway from early endosomes to the TGN was severely impaired in the Cdc50p-depleted *gcs1Δ* mutant. Mislocalization of the TGN resident protein Kex2p in the Cdc50p-depleted *gcs1Δ* mutant could be explained by a default transport system that moves this protein to the vacuole when the transport pathway from early endosomes to the TGN is defective (Lewis *et al*., 2000; Wilcox *et al*., 1992). It, however, is possible

that this defect was indirectly caused by defective TGN-to-early endosome transport, which would affect the function of early endosomes. We believe this was unlikely; Tlg1p, which is recycled between early endosomes and the TGN (Lewis *et al*., 2000), accumulated in the GFP-Snc1p-containing structures, but not in the Sec7p-positive structures, implying that the TGN-to-early endosome transport was not impaired in the Cdc50p-depleted *gcs1Δ* mutant. Our recent results suggest that *CDC50* and *DRS2* are actually involved in the retrieval pathway from early endosomes to the TGN. Genetic data suggest that *CDC50* and *DRS2* are functionally very similar to *RCY1*, which is required for the endocytic recycling pathway, but not for vacuolar protein sorting or the secretory pathway (Wiederkehr *et al*., 2000). Moreover, Cdc50p-Drs2p was coimmunoprecipitated with Rcy1p (Furuta *et al*., our unpublished results). In addition, it has recently been suggested that Gcs1p is involved in the COPI vesicle formation at early endosomes through an interaction with Snc1p and subsequently promoting the Arf1p-GTP recruitment (Robinson *et al*., 2006). Taken together, it seems that the observed defects in the early endosome-to-TGN transport in the Cdc50p-depleted *gcs1Δ* mutant were due to synthetic effects in the same pathway, rather than cumulative defects in multiple pathways. Thus, the Cdc50p-Drs2p putative APLT and Gcs1p may cooperate in vesicle formation at early endosomes.

Possible Involvement of the Cdc50p-Drs2p Putative APLT in the Formation of CCVs or COPI Vesicles at Early Endosomes

We identified *GGA1* and *GGA2* in our search for genes encoding clathrin adaptors that when mutated cause synthetic growth defects with the *cdc50Δ* mutation. Similar to the Cdc50p-depleted *gcs1Δ* mutant, the Cdc50p-depleted *gga1Δ gga2Δ* mutant intracellularly accumulated Snc1p-containing structures, suggesting that the Cdc50p-depleted

gga1Δ gga2Δ mutant is defective in the retrieval pathway from early endosomes to the TGN. Unlike *GCS1*, however, in which null mutation does not affect the rate of CPY maturation, Gga1p and Gga2p are involved in the TGN-to-late endosome transport pathway with clathrin (Costaguta *et al*., 2001). In the *gga1Δ gga2Δ* mutant, the late endosomal protein Pep12p was redirected to early endosomes (Black and Pelham, 2000). Thus, delivery of late endosomal or vacuolar proteins to early endosomes may perturb the normal function of early endosomes. This defect caused by the *gga1Δ gga2Δ* mutation may exacerbate defects in the early endosome-to-TGN transport pathway in the Cdc50p-depleted wild-type strain, although it is also possible that Gga1p and Gga2p are involved in vesicle budding at early endosomes, as has been suggested in mammalian cells (He *et al*., 2005).

AP-1/clathrin and Arf1p have been implicated in the retrieval of Chs3p from early endosomes to the TGN (Valdivia *et al*., 2002). The *apl2Δ* mutation as well as the *cdc50Δ* mutation caused synthetic defects with the *gcs1Δ* mutation in growth and endocytic recycling of Snc1p, although the defects in the *apl2Δ gcs1Δ* mutant were mild compared to those in the Cdc50p-depleted *gcs1Δ* mutant. In addition, like the *cdc50Δ* mutation, the *apl2Δ* mutation causes synthetic growth defects with the *gga1Δ gga2Δ* mutation (Costaguta *et al*., 2001), but not with the *cdc50Δ* mutation (our unpublished results). These results suggest that Cdc50p-Drs2p and AP-1 may be involved in a common step in the early endosome-to-TGN transport pathway. Very recently, the *apl2 gga1 gga2* mutant has been shown to exhibit defects in the early endosome-to-TGN retrieval of a model TGN protein consisting of the cytosolic domain of Ste13p fused to the transmembrane and luminal domains of alkaline phosphatase (Foote and Nothwehr, 2006). Furthermore, the direct interaction of a cytosolic region of Ste13p with AP-1 suggests that Ste13p is recruited into AP-1/clathrin vesicles at early

endosomes (Foote and Nothwehr, 2006). We demonstrated that Apl4p-GFP was localized to endosomal/TGN compartments in a manner dependent on Cdc50p and Gcs1p (Fig. 9). Thus, the Cdc50p-Drs2p putative APLT may promote the formation of AP-1/clathrin vesicles at early endosomes. Localization of Apl2p-GFP to punctate structures was completely abolished by treatment with brefeldin A, an inhibitor for the Arf1 activation (Fernandez and Payne, 2006), consistent with the idea that Gcs1p contributes to the localization of AP-1 to endosomal membranes via regulation of the Arf1p activity.

The *cdc50* null mutant intracellularly accumulates Snc1p (Saito *et al*., 2004), whereas the *apl2Δ* single mutant exhibits an almost wild-type phenotype, implying that Cdc50p-Drs2p is involved in the formation of another type of vesicle. COPI vesicles may be candidates for these vesicles. Several lines of evidence suggest that COPI is also involved in the transport of Snc1p from early endosomes to the TGN (Lewis *et al*., 2000; Cai *et al*., 2005; Robinson *et al*., 2006). *In vitro* studies have suggested that the physical interaction between Snc1p and Gcs1p results in the efficient recruitment of GTP-Arf1p and coatomer to Snc1p (Robinson *et al*., 2006). It is known that Arf GAPs act to dissociate the protein coat from membranes by stimulating GTP hydrolysis and converting Arf1p-GTP to Arf1p-GDP (Tanigawa *et al*., 1993). Recent studies about the COPI-mediated transport pathway, however, suggest that Arf GAPs function as subunits of coat proteins rather than simply Arf inactivators, and that Arf GAP activity is required for the packaging of cargo proteins into COPI vesicles (for review, see Nie and Randazzo, 2006). Therefore, Gcs1p may be directly involved in the formation of COPI vesicles at early endosomes.

It has been proposed that APLTs locally generate phospholipid asymmetry to recruit proteins that promote vesicle formation or to assist membrane deformation for

vesicle budding (Graham, 2004). Interestingly, Gcs1p has an ArfGAP1 Lipid Packing Sensor (ALPS) motif that is thought to recognize curved membranes (Bigay *et al*., 2005). Snc1p physically interacts with Gcs1p (Robinson *et al*., 2006) and Rcy1p (Chen *et al*., 2005), and Rcy1p interacts with the Cdc50p-Drs2p complex (Furuta *et al*., our unpublished results), raising the possibility that these proteins are components of the machinery that initiates vesicle budding at early endosomes. Local phospholipid asymmetry generated by these protein interactions might be utilized to recruit AP-1/clathrin or COPI coatomer to the nascent vesicle budding site.

Acknowledgments

We thank Mamiko Satoh for her instructions for electron microscopy and Masahiko Watanabe for the microtome. We thank Akihiko Nakano, Catherine Jackson, Charles Boone, Gregory Payne, Randy Schekman, Roger Tsien, and Yoshinori Ohsumi for yeast strains, plasmids, and antibodies, and Eriko Itoh for her technical assistance. We thank members of the Tanaka Lab for valuable suggestions over the course of these experiments. This work was supported by Grants-in-Aid for Scientific Research from the Japan Society for the Promotion of Science and the Ministry of Education, Culture, Sports, Science, and Technology of Japan to T. Y. and K. T.

References

Achstetter, T., Franzusoff, A., Field, C., and Schekman, R. 1988. *SEC7* encodes an unusual, high molecular weight protein required for membrane traffic from the yeast Golgi apparatus. *J. Biol. Chem.*, **263**: 11711-11717.

Alder-Baerens, N., Lisman, Q., Luong, L., Pomorski, T., and Holthuis, J.C.M. 2006. Loss of P4 ATPases Drs2p and Dnf3p disrupts aminophospholipid transport and asymmetry in yeast post-Golgi secretory vesicles. *Mol. Biol. Cell*, **17**: 1632-1642.

Ayscough, K.R., Stryker, J., Pokala, N., Sanders, M., Crews, P., and Drubin, D.G. 1997. High rates of actin filament turnover in budding yeast and roles for actin in establishment and maintenance of cell polarity revealed using the actin inhibitor latrunculin-A. *J. Cell Biol.*, **137**: 399-416.

Banta, L.M., Robinson, J.S., Klionsky, D.J., and Emr, S.D. 1988. Organelle assembly in yeast: characterization of yeast mutants defective in vacuolar biogenesis and protein sorting. *J. Cell Biol.*, **107**: 1369-1383.

Bensen, E.S., Costaguta, G., and Payne, G.S. 2000. Synthetic genetic interactions with temperature-sensitive clathrin in *Saccharomyces cerevisiae*: Roles for synaptojanin-like Inp53p and dynamin-related Vps1p in clathrin-dependent protein sorting at the *trans*-Golgi network. *Genetics*, **154**: 83-97.

Bigay, J., Casella, J.F., Drin, G., Mesmin, B., and Antonny, B. 2005. ArfGAP1 responds to membrane curvature through the folding of a lipid packing sensor motif. *EMBO J.*,

24: 2244-2253.

Black, M.W., and Pelham, H.R.B. 2000. A selective transport route from Golgi to late endosomes that requires the yeast GGA proteins. *J. Cell Biol.*, **151**: 587-600.

Blader, I.J., Cope, M.J.T.V., Jackson, T.R., Profit, A.A., Greenwood, A.F., Drubin, D.G., Prestwich, G.D., and Theibert, A.B. 1999. *GCS1*, an Arf guanosine triphosphatase-activating protein in *Saccharomyces cerevisiae*, is required for normal actin cytoskeletal organization in vivo and stimulates actin polymerization in vitro. *Mol. Biol. Cell*, **10**: 581-596.

Boman, A.L., Salo, P.D., Hauglund, M.J., Strand, N.L., Rensink, S.J., and Zhdankina, O. 2002. ADP-ribosylation factor (ARF) interaction is not sufficient for yeast GGA protein function or localization. *Mol. Biol. Cell*, **13**: 3078-3095.

Brachmann, C.B., Davies, A., Cost, G.J., Caputo, E., Li, J., Hieter, P., and Boeke, J.D. 1998. Designer deletion strains derived from *Saccharomyces cerevisiae* S288C: a useful set of strains and plasmids for PCR-mediated gene disruption and other applications. *Yeast*, **14**: 115-132.

Cai, H., Zhang, Y., Pypaert, M., Walker, L., and Ferro-Novick, S. 2005. Mutants in *trs120* disrupt traffic from the early endosome to the late Golgi. *J. Cell Biol.*, **171**: 823-833.

Catty, P., de Kerchove d'Exaerde, A., and Goffeau, A. 1997. The complete inventory of

the yeast *Saccharomyces cerevisiae* P-type transport ATPases. *FEBS Lett.*, **409**: 325-332.

Chantalat, S., Park, S.K., Hua, Z., Liu, K., Gobin, R., Peyroche, A., Rambourg, A., Graham, T.R., and Jackson, C.L. 2004. The Arf activator Gea2p and the P-type ATPase Drs2p interact at the Golgi in *Saccharomyces cerevisiae*. *J. Cell Sci.*, **117**: 711-722.

Chen, C.Y., and Graham, T.R. 1998. An *arf1Δ* synthetic lethal screen identifies a new clathrin heavy chain conditional allele that perturbs vacuolar protein transport in *Saccharomyces cerevisiae*. *Genetics*, **150**: 577-589.

Chen, C.Y., Ingram, M.F., Rosal, P.H., and Graham, T.R. 1999. Role for Drs2p, a P-type ATPase and potential aminophospholipid translocase, in yeast late Golgi function. *J. Cell Biol.*, **147**: 1223-1236.

Chen, S.H., Chen, S., Tokarev, A.A., Liu, F., Jedd, G., and Segev, N. 2005. Ypt31/32 GTPases and their novel F-box effector protein Rcy1 regulate protein recycling. *Mol. Biol. Cell*, **16**: 178-192.

Chuang, J.S., and Schekman, R.W. 1996. Differential trafficking and timed localization of two chitin synthase proteins, Chs2p and Chs3p. *J. Cell Biol.*, **135**: 597-610.

Conibear, E., and Stevens, T.H. 2000. Vps52p, Vps53p, and Vps54p form a novel multisubunit complex required for protein sorting at the yeast late Golgi. *Mol. Biol. Cell*, **11**: 305-323.

Cooper, A.A., and Stevens, T.H. 1996. Vps10p cycles between the late-Golgi and pre-vacuolar compartments in its function as the sorting receptor for multiple yeast vacuolar hydrolases. *J. Cell Biol.*, **133**: 529-541.

Costaguta, G., Stefan, C.J., Bensen, E.S., Emr, S.D., and Payne, G.S. 2001. Yeast Gga coat proteins function with clathrin in Golgi to endosome transport. *Mol. Biol. Cell*, **12**: 1885-1896.

Dell'Angelica, E.C., Puertollano, R., Mullins, C., Aguilar, R.C., Vargas, J.D., Hartnell, L.M., and Bonifacino, J.S. 2000. GGAs: a family of ADP ribosylation factor-binding proteins related to adaptors and associated with the Golgi complex. *J. Cell Biol.*, **149**: 81-93.

Devaux, P.F. 1991. Static and dynamic lipid asymmetry in cell membranes. *Biochemis-try*, **30**: 1163-1173.

Dogic, D., de Chassey, B., Pick, E., Cassel, D., Lefkir, Y., Hennecke, S., Cosson, P., and Letourneur, F. 1999. The ADP-ribosylation factor GTPase-activating protein Glo3p is involved in ER retrieval. *Eur. J. Cell Biol.*, **78**: 305-310.

Donaldson, J.G., and Jackson, C.L. 2000. Regulators and effectors of the ARF GTPases. *Curr. Opin. Cell Biol.*, **12**: 475-482.

Elble, R. 1992. A simple and efficient procedure for transformation of yeasts. *Biotech-*

niques, **13**: 18-20.

Engqvist-Goldstein, A.E., and Drubin, D.G. 2003. Actin assembly and endocytosis: from yeast to mammals. *Annu. Rev. Cell Dev. Biol.*, **19**: 287-332.

Fernandez, G.E., and Payne, G.S. 2006. Laa1p, a conserved AP-1 accessory protein important for AP-1 localization in yeast. *Mol. Biol. Cell*, **17**: 3304-3317.

Foote, C., and Nothwehr, S.F. 2006. The clathrin adaptor complex 1 directly binds to a sorting signal in Ste13p to reduce the rate of its trafficking to the late endosome of yeast. *J. Cell Biol.*, **173**: 615-626.

Franzusoff, A., Lauze, E., and Howell, K.E. 1992. Immuno-isolation of Sec7p-coated transport vesicles from the yeast secretory pathway. *Nature*, **355**: 173-175.

Franzusoff, A., Redding, K., Crosby, J., Fuller, R.S., and Schekman, R. 1991. Localization of components involved in protein transport and processing through the yeast Golgi apparatus. *J. Cell Biol.*, **112**: 27-37.

Fuller, R.S., Sterne, R.E., and Thorner, J. 1988. Enzymes required for yeast prohormone processing. *Annu. Rev. Physiol.*, **50**: 345-362.

Gall, W.E., Geething, N.C., Hua, Z., Ingram, M.F., Liu, K., Chen, S.I., and Graham, T.R. 2002. Drs2p-dependent formation of exocytic clathrin-coated vesicles in vivo. *Curr. Biol.*, **12**: 1623-1627.

Gaynor, E.C., Chen, C.Y., Emr, S.D., and Graham, T.R. 1998. ARF is required for maintenance of yeast Golgi and endosome structure and function. *Mol. Biol. Cell*, **9**: 653-670.

Gietz, R.D., and Woods, R.A. 2002. Transformation of yeast by lithium acetate/single-stranded carrier DNA/polyethylene glycol method. *Methods Enzymol.*, **350**: 87-96.

Guthrie, C., and Fink, G.R., eds. 1991. Guide to Yeast Genetics and Molecular Biology. San Diego, CA: Academic Press.

Graham, T.R. 2004. Flippases and vesicle-mediated protein transport. *Trends Cell Biol.*, **14**: 670-677.

He, X., Li, F., Chang, W.P., and Tang, J. 2005. GGA proteins mediate the recycling pathway of memapsin 2 (BACE). *J. Biol. Chem.*, **280**: 11696-11703.

Hirst, J., Lui, W.W.Y., Bright, N.A., Totty, N., Seaman, M.N.J., and Robinson, M.S. 2000. A family of proteins with γ-adaptin and VHS domains that facilitate trafficking between the trans-Golgi network and the vacuole/lysosome. *J. Cell Biol.*, **149**: 67-80.

Holthuis, J.C.M., and Levine, T.P. 2005. Lipid traffic: floppy drives and a superhighway. *Nat. Rev. Mol. Cell Biol.*, **6**: 209-220.

Holthuis, J.C.M., Nichols, B.J., Dhruvakumar, S., and Pelham, H.R.B. 1998a. Two syntaxin homologues in the TGN/endosomal system of yeast. *EMBO J.*, **17**: 113-126.

Holthuis, J.C.M., Nichols, B.J., and Pelham, H.R.B. 1998b. The syntaxin Tlg1p mediates trafficking of chitin synthase III to polarized growth sites in yeast. *Mol. Biol. Cell*, **9**: 3383-3397.

Hua, Z., Fatheddin, P., and Graham, T.R. 2002. An essential subfamily of Drs2p-related P-type ATPases is required for protein trafficking between Golgi complex and endosomal/vacuolar system. *Mol. Biol. Cell*, **13**: 3162-3177.

Huang, C.F., Chen, C.C., Tung, L., Buu, L.M., and Lee, F.J.S. 2002. The yeast ADP-ribosylation factor GAP, Gcs1p, is involved in maintenance of mitochondrial morphology. *J. Cell Sci.*, **115**: 275-282.

Jackson, C.L., and Casanova, J.E. 2000. Turning on ARF: the Sec7 family of guanine-nucleotide-exchange factors. *Trends Cell Biol.*, **10**: 60-67.

Julius, D., Schekman, R., and Thorner, J. 1984. Glycosylation and processing of pre-pro-α-factor through the yeast secretory pathway. *Cell*, **36**: 309-318.

Kishimoto, T., Yamamoto, T., and Tanaka, K. 2005. Defects in structural integrity of ergosterol and the Cdc50p-Drs2p putative phospholipid translocase cause accumulation of endocytic membranes, onto which actin patches are assembled in yeast. *Mol. Biol. Cell*, **16**: 5592-5609.

Kreis, T.E., Lowe, M., and Pepperkok, R. 1995. COPs regulating membrane traffic. *Annu. Rev. Cell Dev. Biol.*, **11**: 677-706.

Letourneur, F., Gaynor, E.C., Hennecke, S., Demolliere, C., Duden, R., Emr, S.D., Riezman, H., and Cosson, P. 1994. Coatomer is essential for retrieval of dilysine-tagged proteins to the endoplasmic reticulum. *Cell*, **79**: 1199-1207.

Lewis, M.J., Nichols, B.J., Prescianotto-Baschong, C., Riezman, H., and Pelham, H.R.B. 2000. Specific retrieval of the exocytic SNARE Snc1p from early yeast endosomes. *Mol. Biol. Cell*, **11**: 23-38.

Liu, Y.W., Huang, C.F., Huang, K.B., and Lee, F.J.S. 2005. Role for Gcs1p in regulation of Arl1p at *trans*-Golgi compartments. *Mol. Biol. Cell*, **16**: 4024-4033.

Longtine, M.S., McKenzie, A., Demarini, D.J., Shah, N.G., Wach, A., Brachat, A., Philippsen, P., and Pringle, J.R. 1998. Additional modules for versatile and economical PCR-based gene deletion and modification in *Saccharomyces cerevisiae*. *Yeast*, **14**: 953-961.

Marcusson, E.G., Horazdovsky, B.F., Cereghino, J.L., Gharakhanian, E., and Emr, S.D. 1994. The sorting receptor for yeast vacuolar carboxypeptidase Y is encoded by the *VPS10* gene. *Cell*, **77**: 579-586.

Misu, K., Fujimura-Kamada, K., Ueda, T., Nakano, A., Katoh, H., and Tanaka, K. 2003.

Cdc50p, a conserved endosomal membrane protein, controls polarized growth in *Saccharomyces cerevisiae*. *Mol. Biol. Cell*, **14**: 730-747.

Mulholland, J., and Botstein, D. 2002. Immunoelectron microscopy of aldehyde-fixed yeast cells. *Methods Enzymol.*, **351**: 50-81.

Natarajan, P., Wang, J., Hua, Z., and Graham, T.R. 2004. Drs2p-coupled aminophospholipid translocase activity in yeast Golgi membranes and relationship to *in vivo* function. *Proc. Natl. Acad. Sci. USA*, **101**: 10614-10619.

Nie, Z., and Randazzo, P.A. 2006. Arf GAPs and membrane traffic. *J. Cell Sci.*, **119**: 1203-1211.

Panic, B., Whyte, J.R.C., and Munro, S. 2003. The ARF-like GTPases Arl1p and Arl3p act in a pathway that interacts with vesicle-tethering factors at the Golgi apparatus. *Curr. Biol.*, **13**: 405-410.

Peyroche, A., Courbeyrette, R., Rambourg, A., and Jackson, C.L. 2001. The ARF exchange factors Gea1p and Gea2p regulate Golgi structure and function in yeast. *J. Cell Sci.*, **114**: 2241-2253.

Pomorski, T., Holthuis, J.C.M., Herrmann, A., and van Meer, G. 2004. Tracking down lipid flippases and their biological functions. *J. Cell Sci.*, **117**: 805-813.

Pomorski, T., Lombardi, R., Riezman, H., Devaux, P.F., van Meer, G., and Holthuis,

J.C.M. 2003. Drs2p-related P-type ATPases Dnf1p and Dnf2p are required for phospholipid translocation across the yeast plasma membrane and serve a role in endocytosis. *Mol. Biol. Cell*, **14**: 1240-1254.

Poon, P.P., Cassel, D., Spang, A., Rotman, M., Pick, E., Singer, R.A., and Johnston, G.C. 1999. Retrograde transport from the yeast Golgi is mediated by two ARF GAP proteins with overlapping function. *EMBO J.*, **18**: 555-564.

Poon, P.P., Nothwehr, S.F., Singer, R.A., and Johnston, G.C. 2001. The Gcs1 and Age2 ArfGAP proteins provide overlapping essential function for transport from the yeast trans-Golgi network. *J. Cell Biol.*, **155**: 1239-1250.

Poon, P.P., Wang, X., Rotman, M., Huber, I., Cukierman, E., Cassel, D., Singer, R.A., and Johnston, G.C. 1996. *Saccharomyces cerevisiae* Gcs1 is an ADP-ribosylation factor GTPase-activating protein. *Proc. Natl. Acad. Sci. USA*, **93**: 10074-10077.

Robinson, M., Poon, P.P., Schindler, C., Murray, L.E., Kama, R., Gabriely, G., Singer, R.A., Spang, A., Johnston, G.C., and Gerst, J.E. 2006. The Gcs1 Arf-GAP mediates Snc1,2 v-SNARE retrieval to the Golgi in yeast. *Mol. Biol. Cell*, **17**: 1845-1858.

Rose, M.D., Winston, F., and Hieter, P. 1990. Methods in Yeast Genetics: A Laboratory Course Manual. Cold Spring Harbor, NY: Cold Spring Harbor Laboratory Press.

Rothblatt, J., and Schekman, R. 1989. A hitchhiker's guide to analysis of the secretory pathway in yeast. *Methods Cell Biol.*, **32**: 3-36.

Saito, K., Fujimura-Kamada, K., Furuta, N., Kato, U., Umeda, M., and Tanaka, K. 2004. Cdc50p, a protein required for polarized growth, associates with the Drs2p P-type ATPase implicated in phospholipid translocation in *Saccharomyces cerevisiae*. *Mol. Biol. Cell*, **15**: 3418-3432.

Santos, B., and Snyder, M. 1997. Targeting of chitin synthase 3 to polarized growth sites in yeast requires Chs5p and Myo2p. *J. Cell Biol.*, **136**: 95-110.

Sato, K., Sato, M., and Nakano, A. 1997. Rer1p as common machinery for the endoplasmic reticulum localization of membrane proteins. *Proc. Natl. Acad. Sci. USA*, **94**: 9693-9698.

Sato, K., Sato, M., and Nakano, A. 2001. Rer1p, a retrieval receptor for endoplasmic reticulum membrane proteins, is dynamically localized to the Golgi apparatus by coatomer. *J. Cell Biol.*, **152**: 935-944.

Seaman, M.N.J., McCaffery, J.M., and Emr S.D. 1998. A membrane coat complex essential for endosome-to-Golgi retrograde transport in yeast. *J. Cell Biol.*, **142**: 665-681.

Sikorski, R.S., and Hieter, P. 1989. A system of shuttle vectors and yeast host strains designed for efficient manipulation of DNA in *Saccharomyces cerevisiae*. *Genetics*, **122**: 19-27.

Spang, A., Herrmann, J.M., Hamamoto, S., and Schekman, R. 2001. The ADP ribosyla-

tion factor-nucleotide exchange factors Gea1p and Gea2p have overlapping, but not redundant functions in retrograde transport from the Golgi to the endoplasmic reticulum. *Mol. Biol. Cell*, **12**: 1035-1045.

Stearns, T., Kahn, R.A., Botstein, D., and Hoyt, M.A. 1990. ADP ribosylation factor is an essential protein in *Saccharomyces cerevisiae* and is encoded by two genes. *Mol. Cell. Biol.*, **10**: 6690-6699.

Tanigawa, G., Orci, L., Amherdt, M., Ravazzola, M., Helms, J.B., and Rothman, J.E. 1993. Hydrolysis of bound GTP by ARF protein triggers uncoating of Golgi-derived COP-coated vesicles. *J. Cell Biol.*, **123**: 1365-1371.

Valdivia, R.H., Baggott, D., Chuang, J.S., and Schekman, R.W. 2002. The yeast clathrin adaptor protein complex 1 is required for the efficient retention of a subset of late Golgi membrane proteins. *Dev. Cell*, **2**: 283-294.

van Dam, E.M., and Stoorvogel, W. 2002. Dynamin-dependent transferrin receptor recycling by endosome-derived clathrin-coated vesicles. *Mol. Biol. Cell*, **13**: 169-182.

Vida, T.A., and Emr, S.D. 1995. A new vital stain for visualizing vacuolar membrane dynamics and endocytosis in yeast. *J. Cell Biol.*, **128**: 779-792.

Wiederkehr, A., Avaro, S., Prescianotto-Baschong, C., Haguenauer-Tsapis, R., and Riezman, H. 2000. The F-box protein Rcy1p is involved in endocytic membrane traffic and recycling out of an early endosome in *Saccharomyces cerevisiae*. *J. Cell Biol.*, **149**:

397-410.

Wilcox, C.A., Redding, K., Wright, R., and Fuller, R.S. 1992. Mutation of a tyrosine localization signal in the cytosolic tail of yeast Kex2 protease disrupts Golgi retention and results in default transport to the vacuole. *Mol. Biol. Cell*, **3**: 1353-1371.

Wright, R. 2000. Transmission electron microscopy of yeast. Microsc. *Res. Tech.*, **51**: 496-510.

Yahara, N., Ueda, T., Sato, K., and Nakano, A. 2001. Multiple roles of Arf1 GTPase in the yeast exocytic and endocytic pathways. *Mol. Biol. Cell*, **12**: 221-238.

Yanagisawa, L.L., Marchena, J., Xie, Z., Li, X., Poon, P.P., Singer, R.A., Johnston, G.C., Randazzo, P.A., and Bankaitis, V.A. 2002. Activity of specific lipid-regulated ADP ribosylation factor-GTPase-activating proteins is required for Sec14p-dependent Golgi secretory function in yeast. *Mol. Biol. Cell*, **13**: 2193-2206.

Yeung, B.G., and Payne, G.S. 2001. Clathrin interactions with C-terminal regions of the yeast AP-1 β and γ subunits are important for AP-1 association with clathrin coats. *Traffic*, **2**: 565-576.

Yeung, B.G., Phan, H.L., and Payne, G.S. 1999. Adaptor complex-independent clathrin function in yeast. *Mol. Biol. Cell*, **10**: 3643-3659.

Zhang, C.J., Bowzard, J.B., Anido, A., and Kahn, R.A. 2003. Four ARF GAPs in *Sac-*

charomyces cerevisiae have both overlapping and distinct functions. *Yeast*, **20**: 315-330.

Zhdankina, O., Strand, N.L., Redmond, J.M., and Boman, A.L. 2001. Yeast GGA proteins interact with GTP-bound Arf and facilitate transport through the Golgi. *Yeast*, **18**: 1-18.

Ziman, M., Chuang, J.S., and Schekman, R.W. 1996. Chs1p and Chs3p, two proteins involved in chitin synthesis, populate a compartment of the *Saccharomyces cerevisiae* endocytic pathway. *Mol. Biol. Cell*, **7**: 1909-1919.

Table I. *S. cerevisiae* STRAINS USED IN THIS STUDY

Strain[a)]	Genotype	Reference or source
NYY18-2	*MAT*α *ura3 lys2 trp1 his3 leu2 ade2::arf1-18::ADE2 arf1::HIS3 arf2::HIS3*	Yahara *et al*., (2001)
SF821-8A	*MAT*a *ura3-52 leu2-3,112 trp1-289 his4-580a sec7-1*	Achstetter *et al*., (1988)
CJY062-10-2	*MAT*α *ura3-52 leu2-3,112 his3-Δ200 lys2-801 gea1-4 gea2Δ::HIS3MX6*	Peyroche *et al*., (2001)
APY022	*MAT*α *ura3-52 leu2-3,112 his3-Δ200 lys2-801 ade2-101 gea1-6 gea2Δ::HIS3MX6*	Peyroche *et al*., (2001)
APY026	*MAT*a *ura3-52 leu2-3,112 his3-Δ200 gea1-19 gea2Δ::HIS3MX6*	Peyroche *et al*., (2001)
GPY1019-5B	*MAT*a *ura3-52 his3-Δ200 trp1-901 lys2-801 leu2-3,112 suc2-Δ9 chc1-521*	Bensen *et al*., (2000)
MBY6-4D	*MAT*α *ura3-52 leu2-3,112 trp1-289 his3/4 sec21-1*	A gift from Randy Schekman
YEF473	*MAT*a/α *lys2-801*/*lys2-801 ura3-52*/*ura3-52 his3Δ-200*/*his3Δ-200 trp1Δ-63*/*trp1Δ-63 leu2Δ-1*/*leu2Δ-1*	Longtine *et al*., (1998)
BY4743	*MAT*a/α *LYS2*/*lys2Δ0 ura3Δ0*/*ura3Δ0 his3Δ1*/*his3Δ1 leu2Δ0*/*leu2Δ0 met15Δ0/MET15*	Brachmann *et al*., (1998)
YKT38	*MAT*a *lys2-801 ura3-52 his3Δ-200 trp1Δ-63 leu2Δ-1*	Misu *et al*., (2003)

YKT903	*MAT*a *KEX2-EGFP::KanMX6*	This study
YKT905	*MAT*a *SEC7-mRFP1::TRP1*	This study
YKT912	*MAT*α *cdc50Δ::HphMX4*	This study
YKT934	*MAT*α *HphMX4::*P_{GAL1}*-3HA-CDC50*	This study
YKT957	*MAT*α *VPS10-EGFP::KanMX6*	This study
YKT1275	*MAT*a *arf1Δ::KanMX6*	This study
YKT1276	*MAT*a *HphMX4::*P_{GAL1}*-3HA-CDC50 arf1Δ::KanMX6*	This study
YKT1277[b)]	*MAT*α *ura3 lys2 trp1 his3 leu2 ade2::arf1-18::ADE2 arf1::HIS3 arf2::HIS3 KanMX6::*P_{GAL1}*-3HA-CDC50*	This study
YKT1278[b)]	*MAT*α *ura3 lys2 trp1 his3 leu2 ade2::arf1-18::ADE2 arf1::HIS3 arf2::HIS3 SEC7-mRFP1::KanMX6*	This study
YKT1279	*MAT*a *arf1Δ::KanMX6 SEC7-mRFP1::TRP1*	This study
YKT1280	*MAT*a *arf2Δ::KanMX6*	This study
YKT1281	*MAT*a *arf3Δ::KanMX6*	This study
YKT1282	*MAT*a *gcs1Δ::KanMX6*	This study
YKT1283	*MAT*a *glo3Δ::KanMX6*	This study
YKT1284	*MAT*a *gea1Δ::KanMX6*	This study
YKT1285	*MAT*a *gea2Δ::KanMX6*	This study
YKT1286	*MAT*a *HphMX4::*P_{GAL1}*-3HA-CDC50 gcs1Δ::KanMX6*	This study
YKT1287	*MAT*a *HphMX4::*P_{GAL1}*-3HA-CDC50 VPS10-EGFP::KanMX6*	This study
YKT1288	*MAT*a *gcs1Δ::TRP1 VPS10-EGFP::KanMX6*	This study
YKT1289	*MAT*α *HphMX4::*P_{GAL1}*-3HA-CDC50 gcs1Δ::TRP1*	This study

	VPS10-EGFP::KanMX6	
YKT1290	*MAT*α *HphMX4::P_{GAL1}-3HA-CDC50 KEX2-EGFP::KanMX6*	This study
YKT1291	*MAT*α *gcs1Δ::TRP1 KEX2-EGFP::KanMX6*	This study
YKT1292	*MAT*a *HphMX4::P_{GAL1}-3HA-CDC50 gcs1Δ::TRP1 KEX2-EGFP::KanMX6*	This study
YKT1293	*MAT*α *HphMX4::P_{GAL1}-3HA-CDC50 SEC7-mRFP1::TRP1*	This study
YKT1294	*MAT*α *gcs1Δ::KanMX6 SEC7-mRFP1::TRP1*	This study
YKT1295	*MAT*α *HphMX4::P_{GAL1}-3HA-CDC50 gcs1Δ::KanMX6 SEC7-mRFP1::TRP1*	This study
YKT1302	*MAT*a *APL4-EGFP::KanMX6*	This study
YKT1303	*MAT*a *cdc50Δ::HIS3MX6 APL4-EGFP::KanMX6*	This study
YKT1304	*MAT*α *gcs1Δ::TRP1 APL4-EGFP::KanMX6*	This study
YKT1305	*MAT*α *HphMX4::P_{GAL1}-3HA-CDC50 gcs1Δ::TRP1 APL4-EGFP::KanMX6*	This study
YKT1306	*MAT*a *APL4-EGFP::KanMX6 SEC7-mRFP1::TRP1*	This study
KKT2	*MAT*a *lys2Δ0 ura3Δ0 his3Δ1 leu2Δ0 met15Δ0*	Kishimoto *et al*., (2005)
KKT127	*MAT*α *HphMX4::P_{GAL1}-CDC50*	This study
KKT299	*MAT*a *gga1Δ::HIS3MX6*	This study
KKT300	*MAT*a *gga2Δ::KanMX6*	This study
KKT301	*MAT*α *HphMX4::P_{GAL1}-CDC50 gga1Δ::HIS3MX6*	This study
KKT302	*MAT*a *HphMX4::P_{GAL1}-CDC50 gga2Δ::KanMX6*	This study

KKT303	*MAT*a *gga1Δ::HIS3MX6 gga2Δ::KanMX6*	This study
KKT304	*MAT*a *HphMX4::*P_{GAL1}*-CDC50 gga1Δ::HIS3MX6 gga2Δ::KanMX6*	This study
KKT305	*MAT*a *apl2Δ::HphMX4*	This study
KKT306	*MAT*a *gcs1Δ::KanMX6*	This study
KKT307	*MAT*a *apl2Δ::HphMX4 gcs1Δ::KanMX6*	This study

[a)] YKT strains are isogenic derivatives of YEF473, whereas KKT strains are isogenic derivatives of BY4743. For YKT and KKT strains, only relevant genotypes are described.

[b)] YKT1277 and YKT1278 are derivatives of NYY18-2.

Table II. PLASMIDS USED IN THIS STUDY

Plasmid	Characteristics	Reference or source
pRS416-GFP-SNC1	*P_{TPI1}-GFP-SNC1 URA3 CEN*	Lewis *et al*., (2000)
pRS416-GFP-SNC1 (pm)	*P_{TPI1}-GFP-SNC1 (pm) URA3 CEN*	Lewis *et al*., (2000)
pKT1613 [pRS313-GCS1]	*GCS1 HIS3 CEN*	This study
pKT1614 [pRS313-gcs1-R54A]	*gcs1-R54A HIS3 CEN*	This study
pRS313	*HIS3 CEN*	Sikorsiki and Hieter (1989)
pSKY5RER1-0	*P_{TDH3}-EGFP-RER1 URA3 CEN*	Yahara *et al*., (2001)
pRS313-CHS3-GFP	*CHS3-EGFP HIS3 CEN*	Valdivia *et al*., (2002)
pRS315-CHS7	*CHS7 LEU2 CEN*	Valdivia *et al*., (2002)
pKT1563 [pRS416-mRFP1-SNC1]	*P_{TPI1}-mRFP1-SNC1 URA3 CEN*	Kishinoto *et al*., (2005)
pKT1566 [YE-plac181-GFP-TLG1]	*GFP-TLG1 LEU2 2μm*	This study
pKT1564 [pRS416-3HA-SNC1]	*P_{TPI1}-3HA-SNC1 URA3 CEN*	This study

FIGURE LEGENDS

Fig. 1. The *arf1* mutants exhibit defects in endocytic recycling of GFP-Snc1p. (A) Depletion of Cdc50p causes the growth defect in the *arf1Δ* and *arf1-18 arf2Δ* mutants. Wild-type (YKT38; a), P_{GAL1}*-3HA-CDC50* (YKT934; b), *arf1Δ* (YKT1275; c), *arf1-18 arf2Δ* (NYY18-2; d), P_{GAL1}*-3HA-CDC50 arf1Δ* (YKT1276; e), and P_{GAL1}*-3HA-CDC50 arf1-18 arf2Δ* (YKT1277; f) strains were streaked onto a plate containing galactose (YPGA) or glucose (YPDA) as a carbon source, followed by incubation at 30°C for 2 d. (B) Localization of GFP-Snc1p in the *arf1* mutants. Wild-type (YKT38; WT), *arf1-18 arf2Δ* (NYY18-2), and *arf1Δ* (YKT1275) strains carrying pRS416-GFP-SNC1 or pRS416-GFP-SNC1 (pm) were grown to mid-log phase in YPDA medium at 30°C, incubated at 30°C or 37°C for 1 h, and observed immediately by fluorescence microscopy. An arrowhead indicates the ring structure that contain GFP-Snc1p. (C) Localization of Sec7p-mRFP1 in the *arf1* mutants. Wild-type (YKT905; WT), *arf1-18 arf2Δ* (YKT1278), and *arf1Δ* (YKT1279) strains expressing Sec7p-mRFP1 were grown to mid-log phase in YPDA medium at 30°C, incubated at 30°C or 37°C for 1 h, and observed immediately by fluorescence microscopy. Bars, 5 μm.

Fig. 2. *CDC50* exhibits a specific genetic interaction with *GCS1* among Arf GAP genes. (A) Genetic interactions between *CDC50* and genes encoding Arf, Arf-like proteins, or regulators of Arf proteins. The *cdc50Δ* mutant was crossed with the indicated mutants to generate diploids. Diploid cells were sporulated, and synthetic lethality was examined using tetrad analysis at 30°C. (B) Tetrad analyses of progeny derived from crossing the *cdc50Δ* mutant (YKT912) with the indicated Arf GAP mutants. Arrows indicate the positions of double mutant segregants. (C) Construction of a conditional *cdc50Δ gcs1Δ* mutant. Wild-type (YKT38; WT), P_{GAL1}*-3HA-CDC50*

(YKT934), *gcs1Δ* (YKT1282), and P_{GAL1}-*3HA-CDC50 gcs1Δ* (YKT1286) strains were streaked onto a YPGA or YPDA plate, followed by incubation at 30°C for 2 d. (D) Requirement of the Arf GAP activity of Gcs1p for growth of the P_{GAL1}-*3HA-CDC50 gcs1Δ* mutant. pRS313 (vector), pRS313-GCS1 (pKT1613), or pRS313-gcs1-R54A (pKT1614) was introduced into the P_{GAL1}-*3HA-CDC50 gcs1Δ* (YKT1286) mutant. Cells were streaked onto a YPDA plate, followed by incubation at 30°C for 2 d.

Fig. 3. Intracellular vesicle transport in the Cdc50p-depleted *gcs1Δ* mutant. Transport in various vesicle transport pathways was examined in the P_{GAL1}-*3HA-CDC50 gcs1Δ* and control strains described in Fig. 2C. (A) Internalization and transport to the vacuole of FM4-64 in the Cdc50p-depleted *gcs1Δ* mutant. Cells were grown in YPDA at 30°C for 6.5 h, labeled in 32 μM FM4-64 for 30 min at 0°C, and then chased in fresh medium at 30°C for 1 h. (B) CPY processing in the Cdc50p-depleted *gcs1Δ* mutant. Cells were depleted of Cdc50p for 8 h at 30°C, labeled with Trans^{35}S-label for 10 min, and chased for 0, 15, or 30 min. CPY was immunoprecipitated, resolved by SDS-PAGE, and detected by autoradiography. (C) Invertase secretion in the Cdc50p-depleted *gcs1Δ* mutant. After incubation in glucose-containing medium for 8 h at 30°C, wild-type (a), P_{GAL1}-*3HA-CDC50* (b), *gcs1Δ* (c), and P_{GAL1}-*3HA-CDC50 gcs1Δ* (d) strains were labeled with Trans^{35}S-label for 4 min and chased for 0 or 60 min. Secreted and intracellular invertase were separated into external and internal fractions, respectively. Invertase was recovered by immunoprecipitation, and visualized by SDS-PAGE and autoradiography. The band indicated by an arrowhead is non-specific. (D) Localization of GFP-Rer1p in the Cdc50p-depleted *gcs1Δ* mutant. The strains used in Fig. 2C were transformed with a single-copy plasmid containing *GFP-RER1* (pSKY5RER1-0). Cells were grown in YPDA medium at 30°C for 8 h, and observed

by fluorescence microscopy. Bars, 5 μm.

Fig. 4. The Cdc50p-depleted *gcs1Δ* mutant exhibits mislocalization of Kex2p-GFP, but not Vps10p-GFP. (A) Localization of Vps10p-GFP and Kex2p-GFP in the Cdc50p-depleted *gcs1Δ* mutant. A Vps10p-GFP- or Kex2p-GFP-expressing variants of the P_{GAL1}-*3HA-CDC50 gcs1Δ* mutant and control strains described in Fig. 2C were constructed. Cells were grown in YPDA medium at 30°C for 8 h, and observed by fluorescence microscopy. The Vps10p-GFP- and Kex2p-GFP-expressing strains were YKT957 and YKT903 (wild-type; WT), YKT1287 and YKT1290 (P_{GAL1}-*3HA-CDC50*; Cdc50p-depleted), YKT1288 and YKT1291 (*gcs1Δ*), and YKT1289 and YKT1292 (P_{GAL1}-*3HA-CDC50 gcs1Δ*; Cdc50p-depleted *gcs1Δ*), respectively. (B) Kex2p-GFP is mislocalized to the vacuole in the Cdc50p-depleted *gcs1Δ* mutant. Wild-type (YKT903; WT) and P_{GAL1}-*3HA-CDC50 gcs1Δ* (YKT1292; Cdc50p-depleted *gcs1Δ*) cells expressing Kex2p-GFP were grown in YPDA medium at 30°C for 7.5 h, labeled with CellTracker Blue CMAC at 30°C for 30 min, and observed by fluorescence microscopy. Bars, 5 μm.

Fig. 5. The Cdc50p-depleted *gcs1Δ* mutant intracellularly accumulates GFP-Snc1p. (A) Localization of GFP-Snc1p in the Cdc50p-depleted *gcs1Δ* mutant. The strains used in Fig. 2C were transformed with pRS416-GFP-SNC1. Cells were grown in YPDA medium at 30°C for 8 h, and observed by fluorescence microscopy. (B) Effect of the LAT-A treatment on the localization of GFP-Snc1p in the Cdc50p-depleted *gcs1Δ* mutant. Wild-type and P_{GAL1}-*3HA-CDC50 gcs1Δ* cells carrying pRS416-GFP-SNC1 that were grown in YPDA medium at 30°C for 7 h, followed by an additional 1-h culture in the presence (LAT-A) or absence (DMSO) of 100 μM LAT-A, were observed by

fluorescence microscopy. Note that a fraction of GFP-Snc1p was localized to the plasma membrane when the Cdc50p-depleted *gcs1Δ* mutant was treated with LAT-A (arrowhead). Bars, 5 μm.

Fig. 6. Chs3p-GFP and GFP-Tlg1p accumulate in the Snc1p-containing endosomal structures in the Cdc50p-depleted *gcs1Δ* mutant. The strains used in Fig. 2C were transformed with plasmids or reconstructed to express two different GFP- or mRFP1-fused proteins. Cells were grown in YPDA medium at 30°C for 8 h, and observed by fluorescence microscopy. Obtained images were merged to demonstrate the coincidence of the two signals. (A) Colocalization of Chs3p-GFP and mRFP1-Snc1p in the Cdc50p-depleted *gcs1Δ* mutant. The strains were cotransformed with pRS313-CHS3-GFP, pRS315-CHS7, and pRS416-mRFP1-SNC1. pRS315-CHS7 was used to avoid artifactual accumulation of Chs3p in the ER (Valdivia *et al*., 2002). (B) Colocalization of GFP-Tlg1p and mRFP1-Snc1p in the Cdc50p-depleted *gcs1Δ* mutant. The strains were cotransformed with YEplac181-GFP-TLG1 and pRS416-mRFP1-SNC1. (C) Colocalization of GFP-Tlg1p and Sec7p-mRFP1 in the Cdc50p-depleted *gcs1Δ* mutant. YEplac181-GFP-TLG1 was introduced into Sec7p-mRFP1-expressing strains: wild-type (YKT905; WT), P_{GAL1}-*3HA-CDC50* (YKT1293; Cdc50p-depleted), *gcs1Δ* (YKT1294), and P_{GAL1}-*3HA-CDC50 gcs1Δ* (YKT1295; Cdc50p-depleted *gcs1Δ*). Bars, 5 μm.

Fig. 7. Gga1p and Gga2p are required for growth of the *cdc50Δ* mutant. (A) Genetic interactions between *CDC50* and genes coding for a protein that has been implicated in Arf1-mediated or clathrin-coated vesicle budding. The *cdc50Δ* mutant was crossed with the indicated mutants to generate diploids. Diploid cells were sporulated, and

synthetic lethality was examined using tetrad analysis at 30°C. (B) Depletion of Cdc50p causes a growth defect in the *gga*Δ mutants. Wild-type (KKT2; a), P_{GAL1}-*3HA-CDC50* (KKT127; b), *gga1*Δ (KKT299; c), *gga2*Δ (KKT300; d), P_{GAL1}-*3HA-CDC50 gga1*Δ (KKT301; e), P_{GAL1}-*3HA-CDC50 gga2*Δ (KKT302; f), *gga1*Δ *gga2*Δ (KKT303; g), and P_{GAL1}-*3HA-CDC50 gga1*Δ *gga2*Δ (KKT304; h) strains were streaked onto a YPGA or YPDA plate, followed by incubation at 30°C for 2 d. (C) CPY processing in the Cdc50p-depleted *gga*Δ mutants. The strains used in (B) were grown in YPDA for 8 h at 30°C to deplete Cdc50p, labeled with Trans^{35}S-label for 10 min, and chased for 0, 15, or 30 min. CPY was immunoprecipitated, resolved by SDS-PAGE, and detected by autoradiography. The Cdc50p-depleted wild-type, *gga1*Δ, and *gga2*Δ cells exhibited wild-type rates of CPY processing (our unpublished results).

Fig. 8. mRFP1-Snc1p largely colocalizes with GFP-Tlg1p in the Cdc50p-depleted *gga*Δ mutants. The strains used in Fig. 7B were cotransformed with pRS416-mRFP1-SNC1 and YEplac181-GFP-TLG1. Cells were grown in YPDA medium at 30°C for 8 h, and observed by fluorescence microscopy. Obtained images were merged to demonstrate the coincidence of the two signals. The Cdc50p-depleted, *gga1*Δ, and Cdc50p-depleted *gga1*Δ mutants exhibited the wild-type localization pattern of mRFP1-Snc1p and GFP-Tlg1p (our unpublished results). Bar, 5 μm.

Fig. 9. AP-1 is implicated in the early endosome-to-TGN transport. (A) The *apl2*Δ *gcs1*Δ mutant exhibits a slow growth phenotype. Wild-type (KKT2; a), *apl2*Δ (KKT305; b), *gcs1*Δ (KKT306; c), and *apl2*Δ *gcs1*Δ (KKT307; d) strains were streaked onto a YPDA plate, followed by incubation at 30°C or 37°C for 1 d. (B) GFP-Snc1p accumulates in intracellular membrane structures in the *apl2*Δ *gcs1*Δ mutant.

Wild-type (KKT2), *apl2Δ* (KKT305), *gcs1Δ* (KKT306) and *apl2Δ gcs1Δ* (KKT307) strains were transformed with pRS416-GFP-SNC1. Cells were grown to mid-log phase in YPDA medium at 30°C and observed by fluorescence microscopy. (C) Localization of Apl4p-GFP to TGN-independent structures. Wild-type cells co--expressing Apl4p-GFP and Sec7p-mRFP1 (YKT1306) were grown to mid-log phase in YPDA medium at 30°C, and observed by fluorescence microscopy. An arrowhead indicates the Apl4p-GFP structure that does not contain Sec7p-mRFP1. (D) Staining Apl4p-GFP-expressing cells with FM4-64. Wild-type cells expressing Apl4p-GFP (YKT1302) were grown in YPDA to late-log phase at 30°C, labeled in 32 μM FM4-64 for 30 min at 0°C, chased in SD medium for 3 min at 30°C, and observed immediately by fluorescence microscopy. An arrowhead indicates the Apl4p-GFP structure that is labeled with FM4-64. (E) Localization of Apl4p-GFP in the Cdc50p-depleted *gcs1Δ* mutant. Wild-type (YKT1302; WT), *cdc50Δ* (YKT1303), *gcs1Δ* (YKT1304), and P_{GAL1}*-3HA-CDC50 gcs1Δ* (YKT1305; Cdc50p-depleted *gcs1Δ*) strains expressing Apl4p-GFP were grown in YPDA medium at 30°C for 8 h, and observed by fluorescence microscopy. In (C) and (D), obtained images were merged to demonstrate the coincidence of the two signals. Bars, 5 μm.

Fig. 10. Accumulation of abnormal membrane structures in the Cdc50p-depleted *gcs1Δ* mutant. (A) Electron microscopic observation of the Cdc50p-depleted *gcs1Δ* mutant. Strains used in Fig. 2C were grown in YPDA medium at 30°C for 8 h, fixed with glutaraldehyde-osmium, and processed for electron microscopic observation. For the Cdc50p-depleted *gcs1Δ* mutant, higher magnification photographs of the areas surrounded by dashed lines are presented to the right side of the panels. Bars, 1 μm and 400 nm for the lower and higher magnification images, respectively. (B) Im-

muno-electron microscopic observation of the Cdc50p-depleted *gcs1Δ* mutant expressing 3HA-Snc1p. The P_{GAL1}-*3HA-CDC50 gcs1Δ* mutant (YKT1286) harboring pRS416-3HA-SNC1 was grown in YPDA medium at 30°C for 8 h, fixed, and processed for immuno-electron microscopic observation. Mouse anti-HA antibodies and 10-nm gold-conjugated anti-mouse IgG antibodies were used as primary and secondary antibodies, respectively. Arrows indicate representatives of the 3HA-Snc1p-positive membrane structures. Bar, 200 nm.

Fig. 11. Accumulation of intracellular membrane structures in the Cdc50p-depleted *ggaΔ* and *apl2Δ gcs1Δ* mutants. (A) Electron microscopic observation of the Cdc50p-depleted *ggaΔ* mutants. The *gga1Δ gga2Δ* (YKT1300) and P_{GAL1}-*3HA-CDC50 gga1Δ gga2Δ* (YKT1301) mutant cells were grown in YPDA medium at 30°C for 8 h, fixed with glutaraldehyde-osmium, and processed the electron microscopic observation. (B) Electron microscopic observation of the *apl2Δ gcs1Δ* mutant. The *apl2Δ gcs1Δ* (KKT307) mutant cells were grown to early logarithmic phase in YPDA medium at 30°C, and processed as described in (A). Bars, 1 μm.

Fig. 1 Sakane et al.

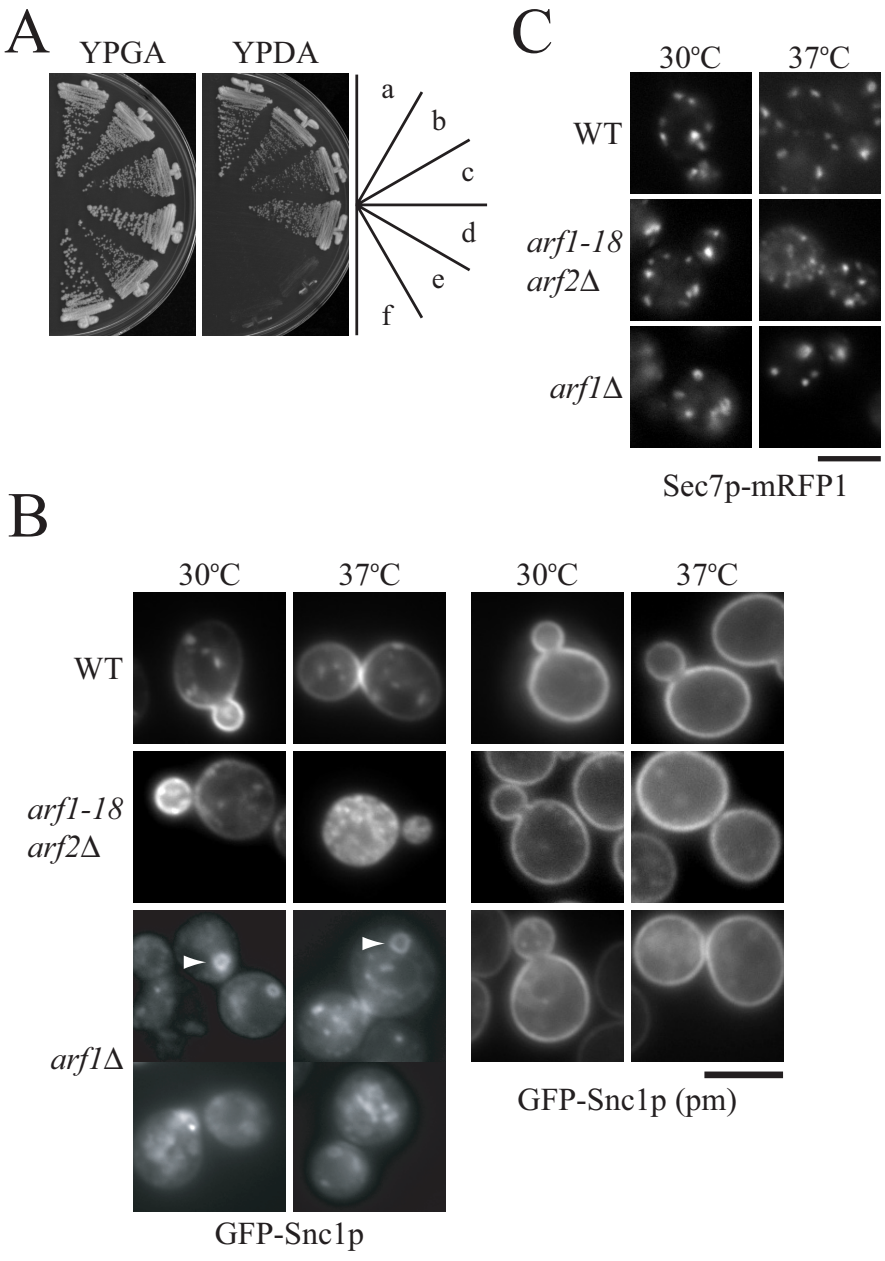

Fig. 2 Sakane et al.

A

Genetic interactions with the *cdc50*Δ mutation

Function	Inviable	Viable
Arf	*arf1*Δ	*arf2*Δ, *arf3*Δ, *arl1*Δ, *arl3*Δ
Arf GAP	*gcs1*Δ	*glo3*Δ, *age1*Δ, *age2*Δ
Arf GEF		*sec7-1*, *syt1*Δ, *gea1*Δ, *gea2*Δ, *gea1-4 gea2*Δ, *gea1-6 gea2*Δ, *gea1-19 gea2*Δ

B

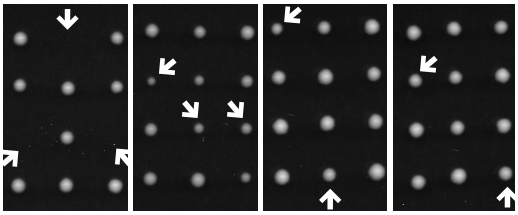

C

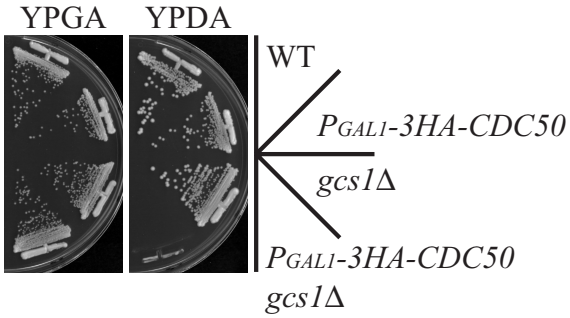

D

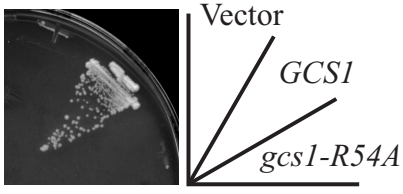

Fig. 3 Sakane et al.

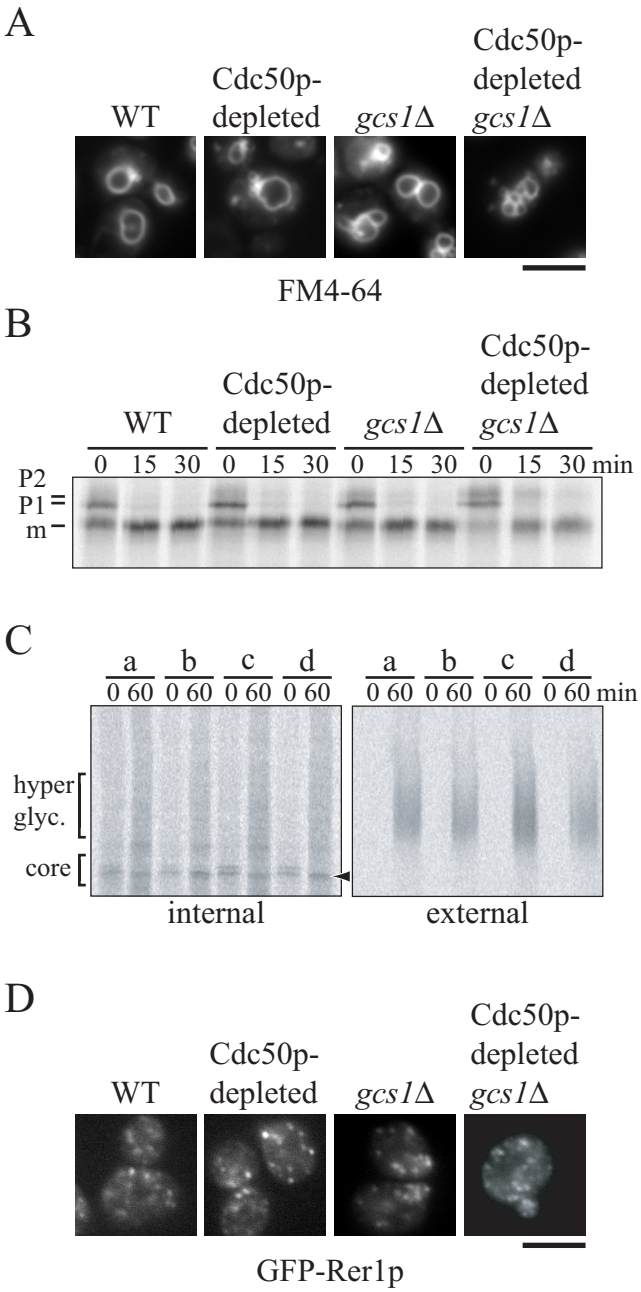

Fig. 4 Sakane et al.

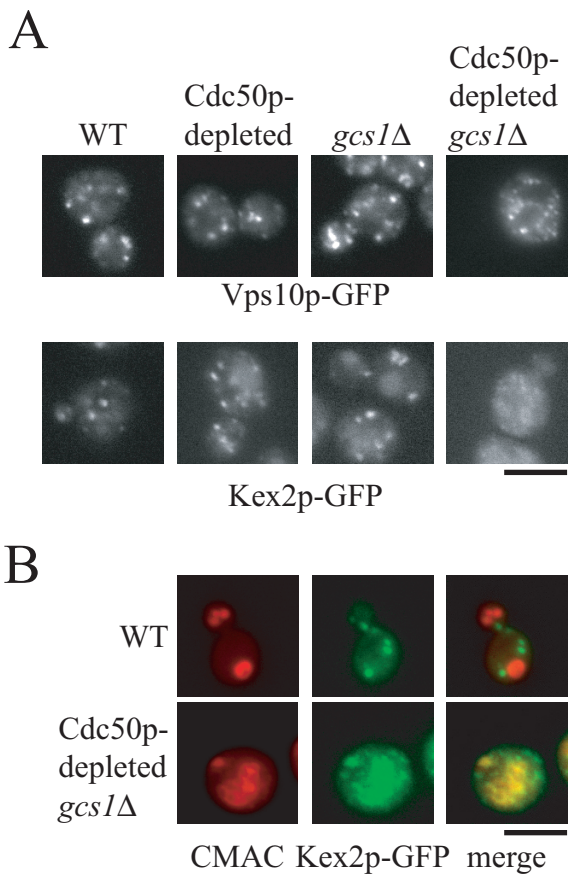

Fig. 5 Sakane et al.

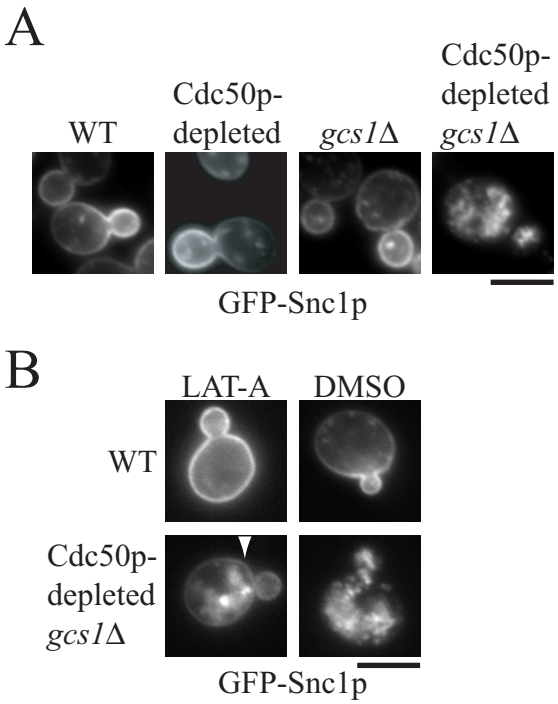

Figure 6 Sakane et al.

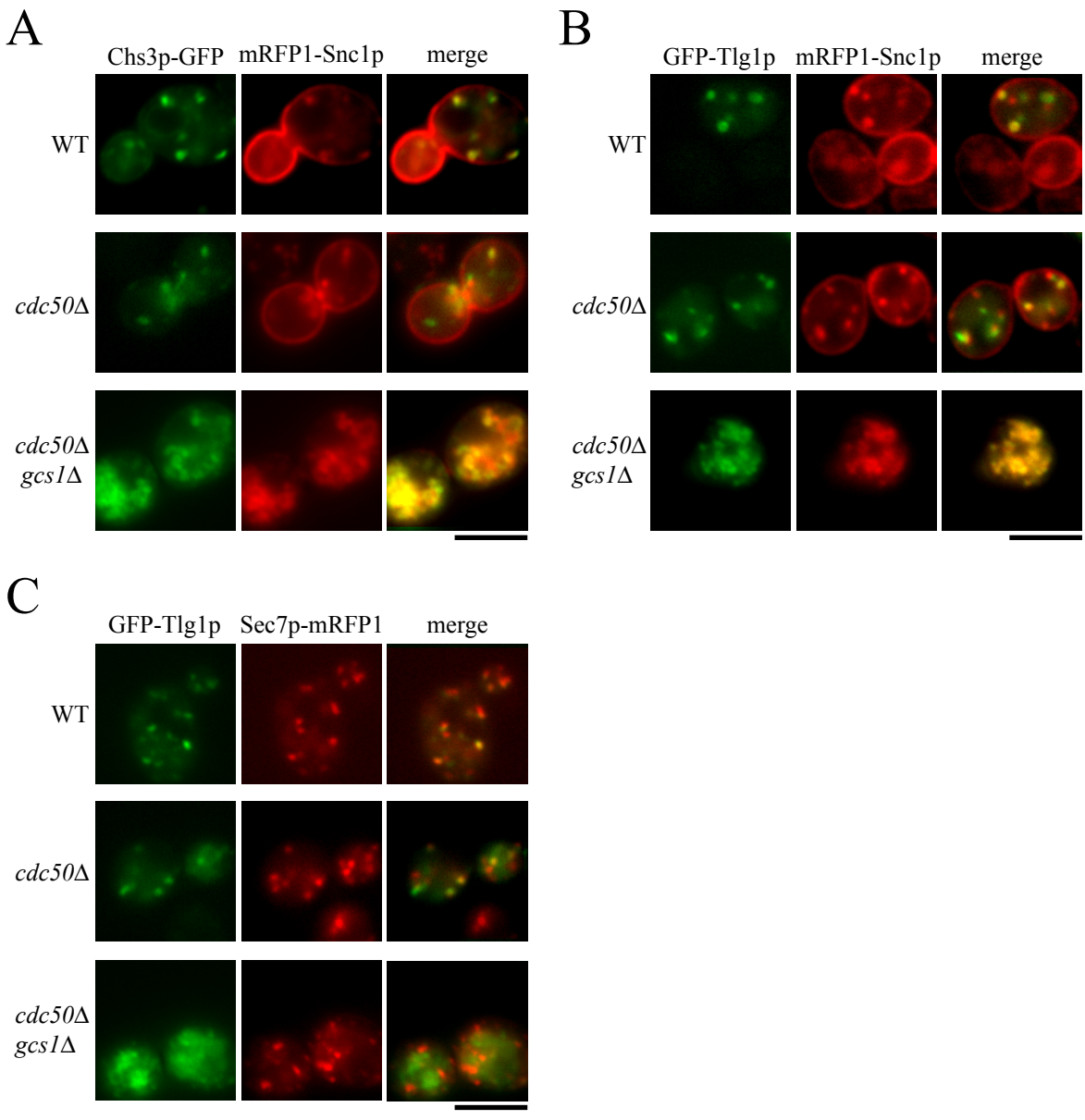

Fig. 7 Sakane et al.

A

Genetic interactions with the *cdc50*Δ mutation

Function	Inviable	Viable
Coat protein	*chc1-521*	*sec21-1*
Adaptor protein	*gga1*Δ *gga2*Δ	*gga1*Δ, *gga2*Δ, *apl2*Δ, *apl4*Δ, *apm1*Δ, *aps1*Δ, *apl5*Δ, *apl6*Δ, *apm3*Δ, *aps3*Δ

B

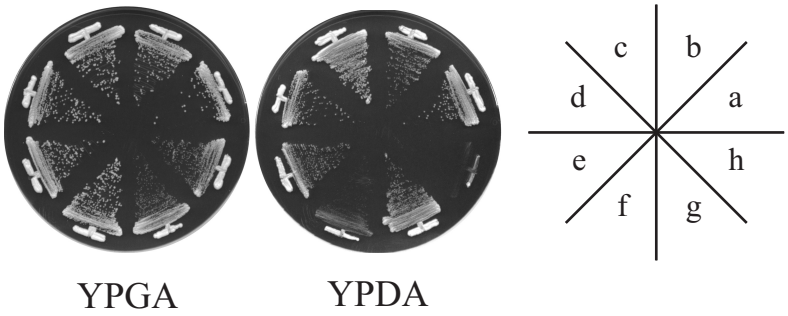

C

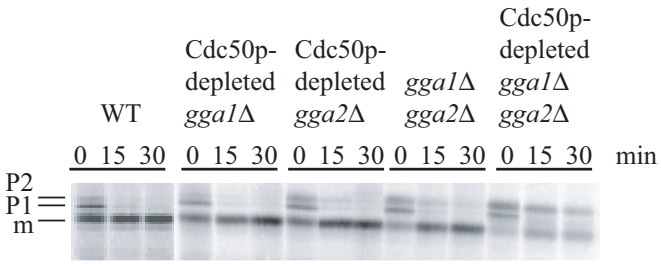

Figure 8 Sakane et al.

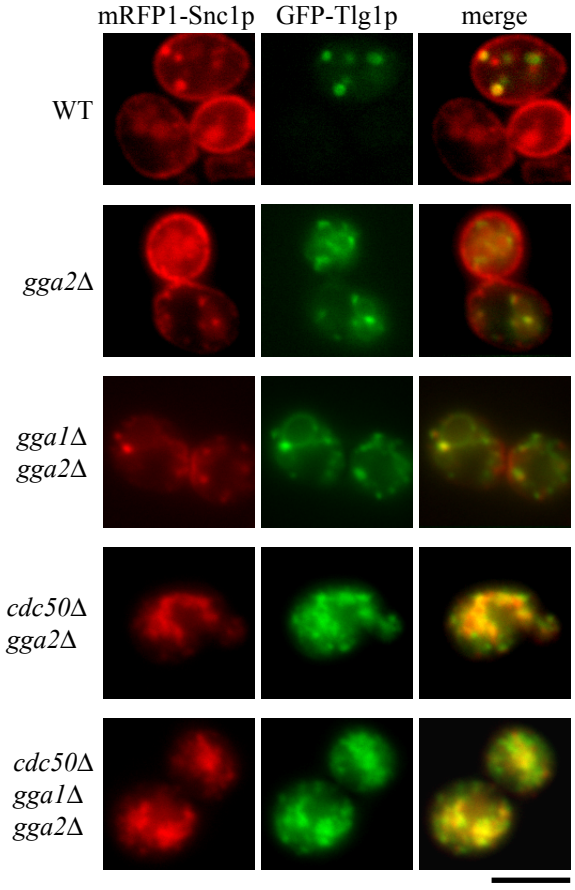

Fig. 9 Sakane et al.

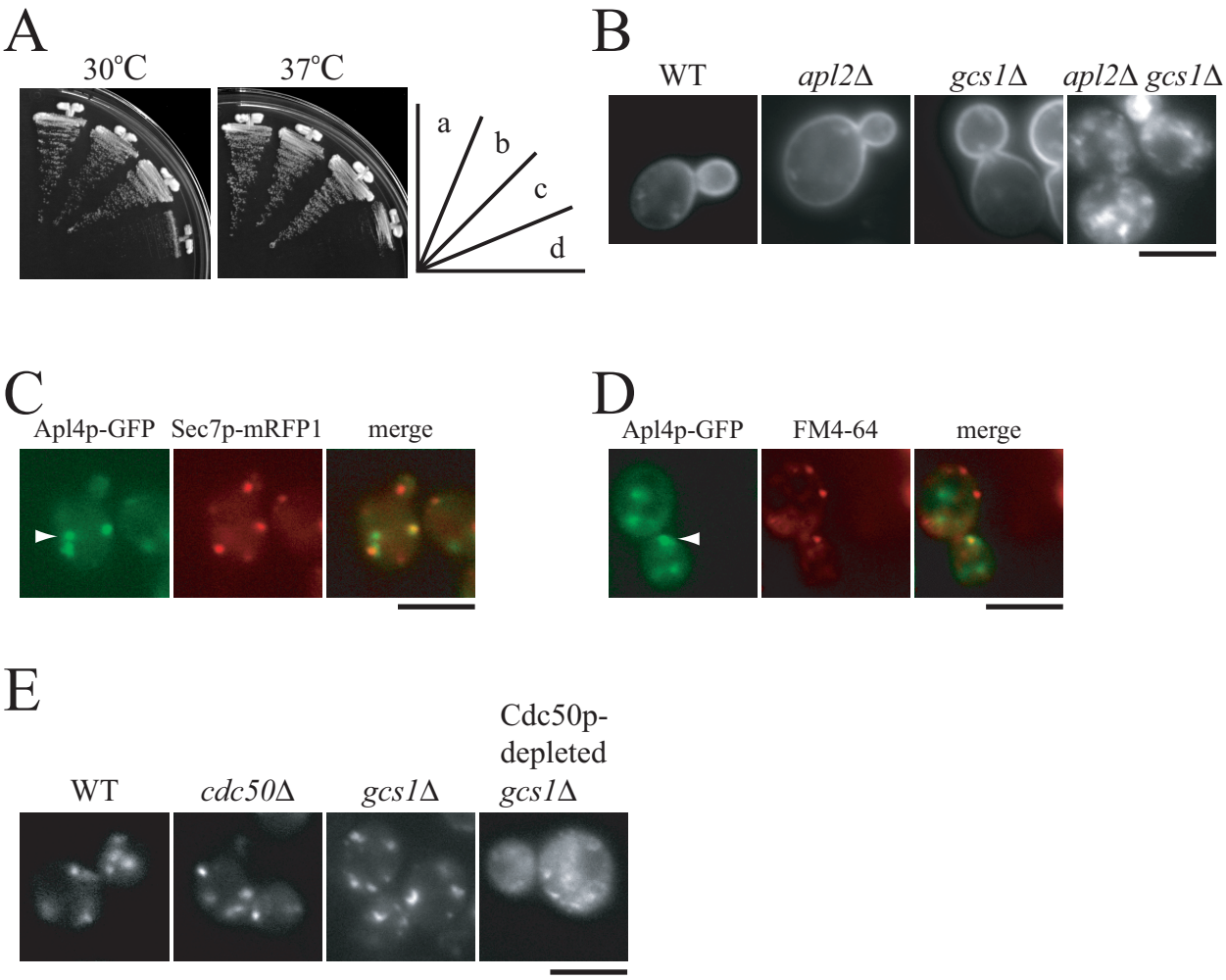

Fig. 10 Sakane et al.

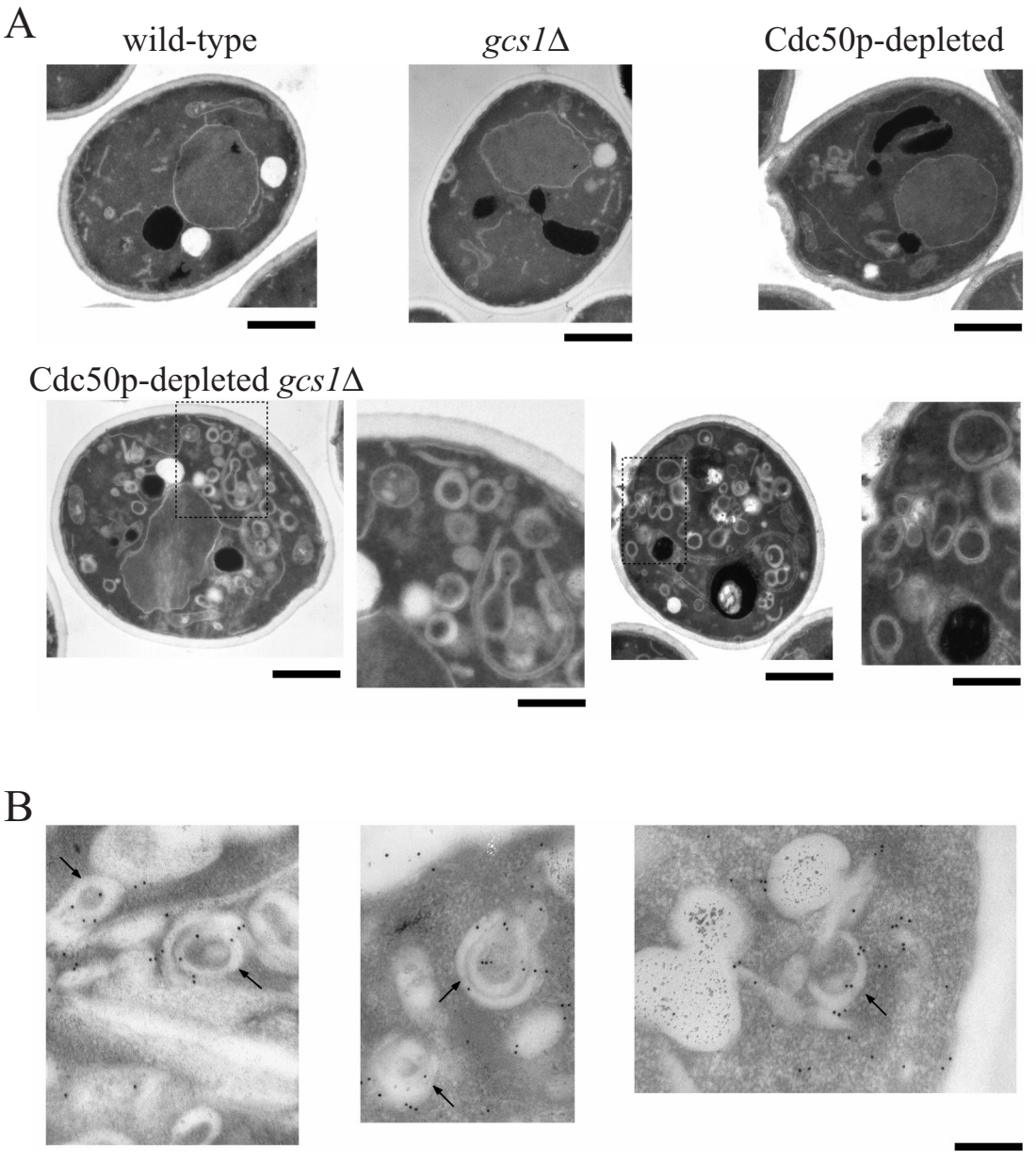

Fig. 11 Sakane et al.